

Final Report

Majority Voting Mechanical Feedback  
Servoactuator for the Saturn S-IV B

Performed Under

NASA Contract NAS8-11634

by

Moog Servocontrols, Inc.  
East Aurora, New York

Report Date - July 22, 1965

1.0 INTRODUCTION

Contract NAS8-11634 was awarded to Moog Servocontrols, Inc. on July 6, 1965. The scope of work was defined as follows: "The contractor shall design, develop, fabricate, test and deliver two (2) each servoactuators of the same configuration and meeting the same basic requirements as the Moog Model 17-189 S-IV B servoactuators. These actuators shall employ redundancy techniques to improve reliability."

The following sections describe the successful fulfillment of the contract objectives.

## 2.0 SUMMARY

The design, development, fabrication, test and delivery of two servoactuators to the basic S-IV B requirements has been completed. These actuators employ redundancy by a technique known as "majority voting." Thru the use of this technique, pertinent output characteristics remain essentially unchanged in consequence to a single failure in any one of the three channels employed. Maximum null offset (due to a failure in a single channel) on the servoactuators built under this contract was less than 4%. This compares very favorably with an initially stated goal of less than 5.0%. The results of testing and evaluating indicate that these limits could be maintained in production thru the use of existing production set-up and test techniques.

Simulator tests indicated adequate performance to the S-IV B requirements. Performance remained adequate with the introduction of simulated failures. Temperature testing to 275°F likewise indicated no adverse performance characteristics.

The observed characteristics of the servoactuators developed under Contract NAS8-11634 are very encouraging with respect to providing redundancy in a servoactuator. In order to evaluate the servoactuators fully, under failure conditions, a larger analysis and test program (than that covered by this contract) is required. Accordingly, an additional contract, NAS8-11998, has been awarded to Moog. This contract covers a reliability analysis, a computer analysis, and an actual induced (not simulated) failure test program.

The following sections describe the actuator design and contain data from tests conducted on the majority voting servoactuators.

### 3.0 DESIGN DESCRIPTION

#### 3.1 General

The Model 17-204 majority voting servoactuator produced under this contract is intended for thrust vector control in the Saturn S-IV B stage. The design has the same hydraulic power capacity (piston area and velocity), and physically will attach to the same clevis fittings as the Model 17-189 actuator presently being produced for the S-IV B.

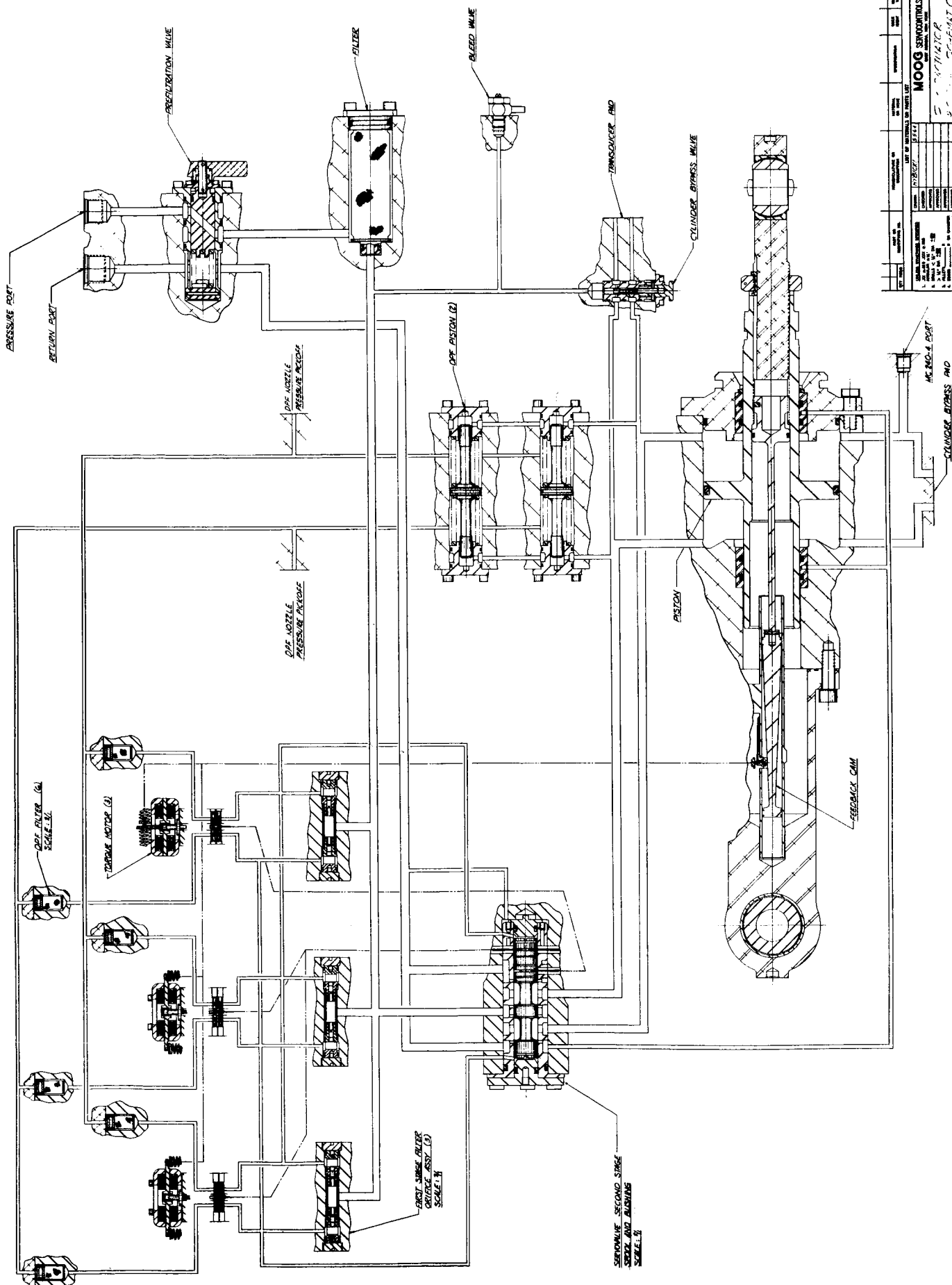
The actuator uses a tapered cylindrical cam for mechanical position feedback and dynamic pressure feedback (DPF) for stabilization of the engine inertia. These features are functionally identical to the current S-IV B actuator. Other similarities to the present S-IV B actuator include: same valve torque motor, same cantilever cam follower assembly, and same accessory components (prefiltration valve, cylinder bypass valve, mid-stroke lock, and vernier scale).

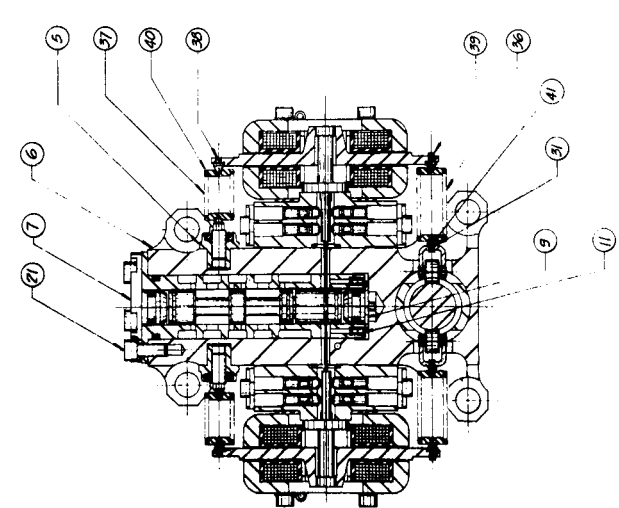
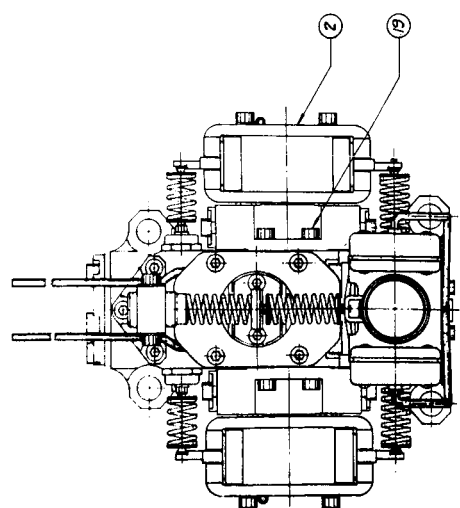
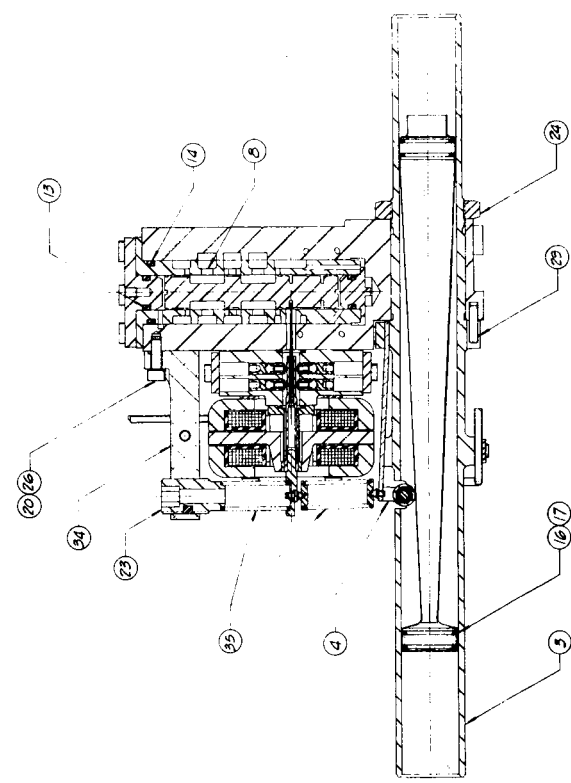
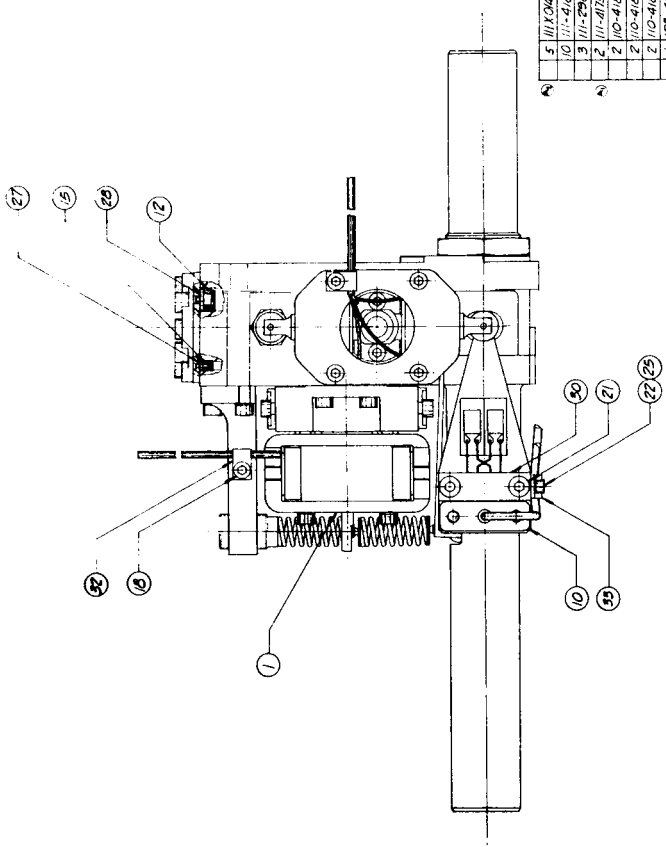
A Pictorial Schematic, 007-41636; Servovalve Assembly Drawing, 010-41833; Servoactuator Assembly Drawing, 010-41933; and Servoactuator Installation Drawing, 001-41932, are included in this report on pages 3-2, 3-3, 3-4, 3-5, and 3-6.

#### 3.2 Operation

The actuator uses three active torque motors in a majority voting configuration. The three torque motors may be driven from a single amplifier, or driven by three separate amplifiers if majority voting is desired for the electrical amplifiers and connecting cables. Each torque motor receives actuator feedback from the cam through separate springs and cam follower assemblies. Each torque motor also receives feedback from the second stage spool. The latter feedbacks are provided by means of cantilever springs attached to each flapper and driven by the single second stage spool of the servovalve. Majority voting is an arrangement whereby the servovalve will behave as the majority of the first stage torque motor hydraulic amplifiers dictate. Since three first stage assemblies are employed, a majority decision will exist when at least two of the first stages

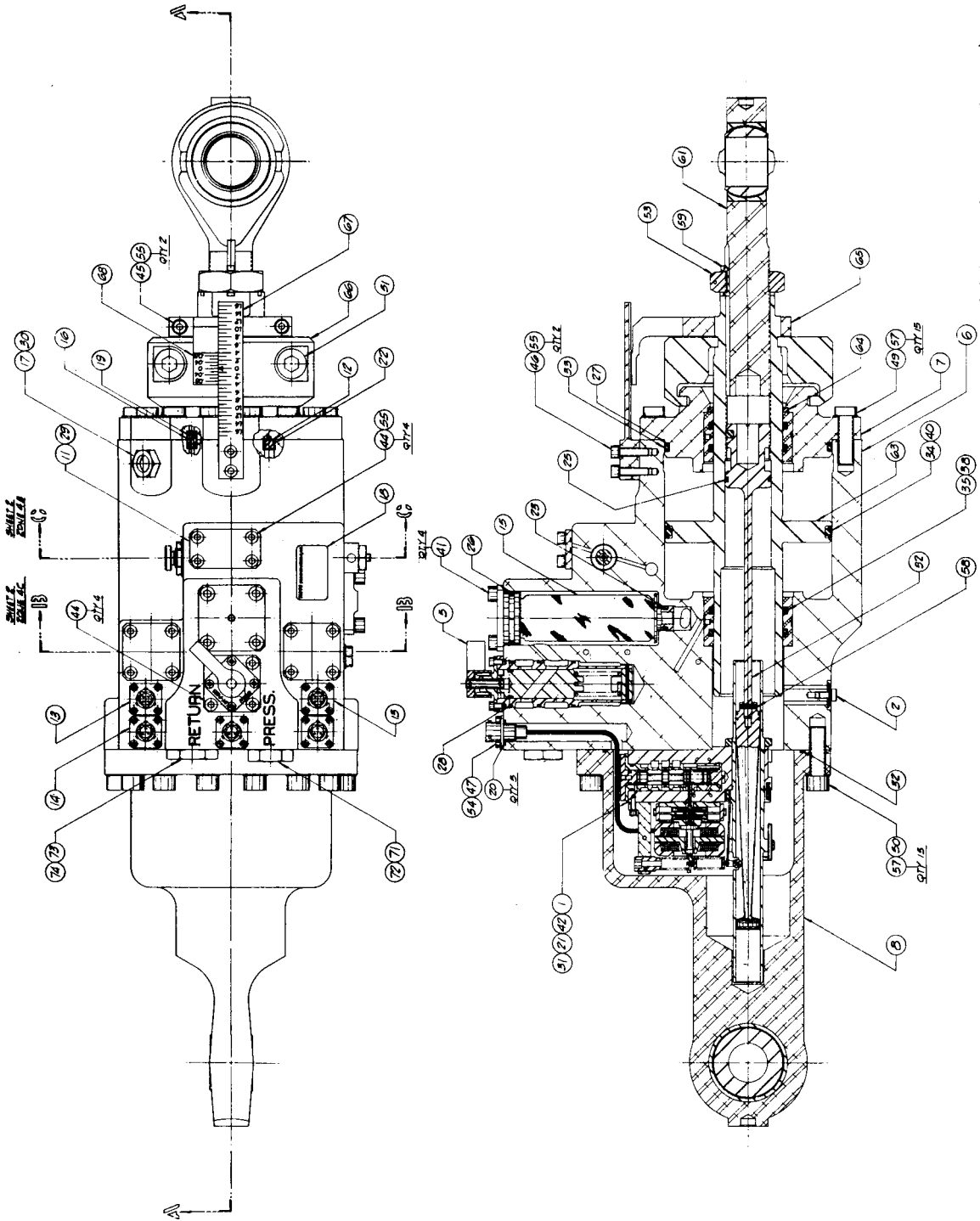






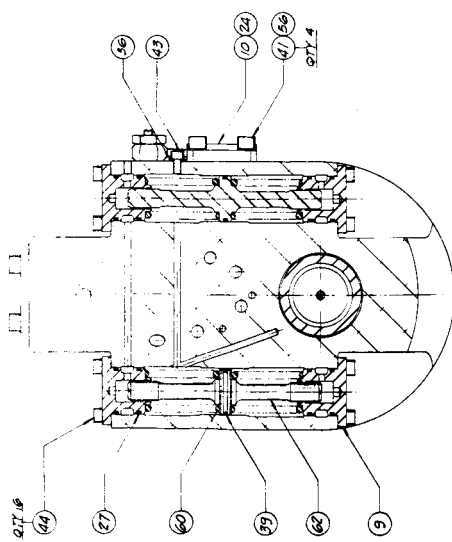
QTY	ITEM NO.	DESCRIPTION	UNIT	QTY
1	111-41852	SEAT SPRING		41
3	111-41853	PIVOT ECCENTRIC		40
2	111-41854	PIVOT		39
2	111-41855	SPRING		38
2	110-41856	SPRING		37
2	110-41857	SPRING		36
1	103-41858	BRACKET		35
2	103-41859	CLAMP		34
3	102-41860	SHIM		33
1	102-41861	RETAINER FOLLOWER		32
1	102-41862	DOINEL		31
2	102-41863	PLUG		30
2	102-41864	PLUG		29
3	102-41865	WASHER		28
2	102-41866	WASHER		27
1	101-41867	NUT RETAINING		26
1	100-41868	ADJUSTOR		25
2	100-41869	SCREW CAP SCH		24
11	100-41870	SCREW CAP SCH		23
3	100-41871	SCREW CAP SCH		22
2	100-41872	SCREW CAP SCH		21
4	100-41873	SCREW CAP SCH		20
2	100-41874	SCREW CAP SCH		19
4	100-41875	SCREW CAP SCH		18
2	100-41876	SCREW CAP SCH		17
2	100-41877	SCREW CAP SCH		16
2	100-41878	SCREW CAP SCH		15
2	100-41879	SCREW CAP SCH		14
2	100-41880	SCREW CAP SCH		13
2	100-41881	SCREW CAP SCH		12
2	100-41882	SCREW CAP SCH		11
2	100-41883	SCREW CAP SCH		10
2	100-41884	SCREW CAP SCH		9
2	100-41885	SCREW CAP SCH		8
2	100-41886	SCREW CAP SCH		7
2	100-41887	SCREW CAP SCH		6
2	100-41888	SCREW CAP SCH		5
2	100-41889	SCREW CAP SCH		4
2	100-41890	SCREW CAP SCH		3
2	100-41891	SCREW CAP SCH		2
2	100-41892	SCREW CAP SCH		1

MOOG SERVOVALVES, INC.  
 SERVOVALVE ASSEMBLY  
 MODEL 16-147  
 94697 E 010-41833  
 11-1-61

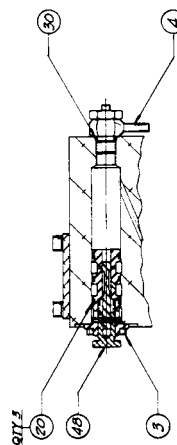


SECTION A-A

MOOG SERVO VALVE ASSEMBLY		010-41933
SERVOACTUATOR ASSEMBLY		010-41933
MODEL 17X204		010-41933
94897		010-41933
MOOG SERVO VALVE ASSEMBLY		010-41933
SERVOACTUATOR ASSEMBLY		010-41933
MODEL 17X204		010-41933
94897		010-41933
MOOG SERVO VALVE ASSEMBLY		010-41933
SERVOACTUATOR ASSEMBLY		010-41933
MODEL 17X204		010-41933
94897		010-41933



SECTION 13-13  
ROTATED 90° COUNTER-CLOCKWISE



PARTIAL  
SECTION 13-13  
ROTATED 90° COUNTER-CLOCKWISE

1	000-20485-0	1" RING	74
2	000-20485-1	1" RING	75
3	000-20485-2	1" RING	76
4	000-20485-3	1" RING	77
5	000-20485-4	1" RING	78
6	000-20485-5	1" RING	79
7	000-20485-6	1" RING	80
8	000-20485-7	1" RING	81
9	000-20485-8	1" RING	82
10	000-20485-9	1" RING	83
11	000-20485-10	1" RING	84
12	000-20485-11	1" RING	85
13	000-20485-12	1" RING	86
14	000-20485-13	1" RING	87
15	000-20485-14	1" RING	88
16	000-20485-15	1" RING	89
17	000-20485-16	1" RING	90
18	000-20485-17	1" RING	91
19	000-20485-18	1" RING	92
20	000-20485-19	1" RING	93
21	000-20485-20	1" RING	94
22	000-20485-21	1" RING	95
23	000-20485-22	1" RING	96
24	000-20485-23	1" RING	97
25	000-20485-24	1" RING	98
26	000-20485-25	1" RING	99
27	000-20485-26	1" RING	100
28	000-20485-27	1" RING	101
29	000-20485-28	1" RING	102
30	000-20485-29	1" RING	103
31	000-20485-30	1" RING	104
32	000-20485-31	1" RING	105
33	000-20485-32	1" RING	106
34	000-20485-33	1" RING	107
35	000-20485-34	1" RING	108
36	000-20485-35	1" RING	109
37	000-20485-36	1" RING	110
38	000-20485-37	1" RING	111
39	000-20485-38	1" RING	112
40	000-20485-39	1" RING	113
41	000-20485-40	1" RING	114
42	000-20485-41	1" RING	115
43	000-20485-42	1" RING	116
44	000-20485-43	1" RING	117
45	000-20485-44	1" RING	118
46	000-20485-45	1" RING	119
47	000-20485-46	1" RING	120
48	000-20485-47	1" RING	121
49	000-20485-48	1" RING	122
50	000-20485-49	1" RING	123
51	000-20485-50	1" RING	124
52	000-20485-51	1" RING	125
53	000-20485-52	1" RING	126
54	000-20485-53	1" RING	127
55	000-20485-54	1" RING	128
56	000-20485-55	1" RING	129
57	000-20485-56	1" RING	130
58	000-20485-57	1" RING	131
59	000-20485-58	1" RING	132
60	000-20485-59	1" RING	133
61	000-20485-60	1" RING	134
62	000-20485-61	1" RING	135
63	000-20485-62	1" RING	136
64	000-20485-63	1" RING	137
65	000-20485-64	1" RING	138
66	000-20485-65	1" RING	139
67	000-20485-66	1" RING	140
68	000-20485-67	1" RING	141
69	000-20485-68	1" RING	142
70	000-20485-69	1" RING	143
71	000-20485-70	1" RING	144
72	000-20485-71	1" RING	145
73	000-20485-72	1" RING	146
74	000-20485-73	1" RING	147
75	000-20485-74	1" RING	148
76	000-20485-75	1" RING	149
77	000-20485-76	1" RING	150
78	000-20485-77	1" RING	151
79	000-20485-78	1" RING	152
80	000-20485-79	1" RING	153
81	000-20485-80	1" RING	154
82	000-20485-81	1" RING	155
83	000-20485-82	1" RING	156
84	000-20485-83	1" RING	157
85	000-20485-84	1" RING	158
86	000-20485-85	1" RING	159
87	000-20485-86	1" RING	160
88	000-20485-87	1" RING	161
89	000-20485-88	1" RING	162
90	000-20485-89	1" RING	163
91	000-20485-90	1" RING	164
92	000-20485-91	1" RING	165
93	000-20485-92	1" RING	166
94	000-20485-93	1" RING	167
95	000-20485-94	1" RING	168
96	000-20485-95	1" RING	169
97	000-20485-96	1" RING	170
98	000-20485-97	1" RING	171
99	000-20485-98	1" RING	172
100	000-20485-99	1" RING	173
101	000-20485-100	1" RING	174
102	000-20485-101	1" RING	175
103	000-20485-102	1" RING	176
104	000-20485-103	1" RING	177
105	000-20485-104	1" RING	178
106	000-20485-105	1" RING	179
107	000-20485-106	1" RING	180
108	000-20485-107	1" RING	181
109	000-20485-108	1" RING	182
110	000-20485-109	1" RING	183
111	000-20485-110	1" RING	184
112	000-20485-111	1" RING	185
113	000-20485-112	1" RING	186
114	000-20485-113	1" RING	187
115	000-20485-114	1" RING	188
116	000-20485-115	1" RING	189
117	000-20485-116	1" RING	190
118	000-20485-117	1" RING	191
119	000-20485-118	1" RING	192
120	000-20485-119	1" RING	193
121	000-20485-120	1" RING	194
122	000-20485-121	1" RING	195
123	000-20485-122	1" RING	196
124	000-20485-123	1" RING	197
125	000-20485-124	1" RING	198
126	000-20485-125	1" RING	199
127	000-20485-126	1" RING	200
128	000-20485-127	1" RING	201
129	000-20485-128	1" RING	202
130	000-20485-129	1" RING	203
131	000-20485-130	1" RING	204
132	000-20485-131	1" RING	205
133	000-20485-132	1" RING	206
134	000-20485-133	1" RING	207
135	000-20485-134	1" RING	208
136	000-20485-135	1" RING	209
137	000-20485-136	1" RING	210
138	000-20485-137	1" RING	211
139	000-20485-138	1" RING	212
140	000-20485-139	1" RING	213
141	000-20485-140	1" RING	214
142	000-20485-141	1" RING	215
143	000-20485-142	1" RING	216
144	000-20485-143	1" RING	217
145	000-20485-144	1" RING	218
146	000-20485-145	1" RING	219
147	000-20485-146	1" RING	220
148	000-20485-147	1" RING	221
149	000-20485-148	1" RING	222
150	000-20485-149	1" RING	223
151	000-20485-150	1" RING	224
152	000-20485-151	1" RING	225
153	000-20485-152	1" RING	226
154	000-20485-153	1" RING	227
155	000-20485-154	1" RING	228
156	000-20485-155	1" RING	229
157	000-20485-156	1" RING	230
158	000-20485-157	1" RING	231
159	000-20485-158	1" RING	232
160	000-20485-159	1" RING	233
161	000-20485-160	1" RING	234
162	000-20485-161	1" RING	235
163	000-20485-162	1" RING	236
164	000-20485-163	1" RING	237
165	000-20485-164	1" RING	238
166	000-20485-165	1" RING	239
167	000-20485-166	1" RING	240
168	000-20485-167	1" RING	241
169	000-20485-168	1" RING	242
170	000-20485-169	1" RING	243
171	000-20485-170	1" RING	244
172	000-20485-171	1" RING	245
173	000-20485-172	1" RING	246
174	000-20485-173	1" RING	247
175	000-20485-174	1" RING	248
176	000-20485-175	1" RING	249
177	000-20485-176	1" RING	250
178	000-20485-177	1" RING	251
179	000-20485-178	1" RING	252
180	000-20485-179	1" RING	253
181	000-20485-180	1" RING	254
182	000-20485-181	1" RING	255
183	000-20485-182	1" RING	256
184	000-20485-183	1" RING	257
185	000-20485-184	1" RING	258
186	000-20485-185	1" RING	259
187	000-20485-186	1" RING	260
188	000-20485-187	1" RING	261
189	000-20485-188	1" RING	262
190	000-20485-189	1" RING	263
191	000-20485-190	1" RING	264
192	000-20485-191	1" RING	265
193	000-20485-192	1" RING	266
194	000-20485-193	1" RING	267
195	000-20485-194	1" RING	268
196	000-20485-195	1" RING	269
197	000-20485-196	1" RING	270
198	000-20485-197	1" RING	271
199	000-20485-198	1" RING	272
200	000-20485-199	1" RING	273
201	000-20485-200	1" RING	274
202	000-20485-201	1" RING	275
203	000-20485-202	1" RING	276
204	000-20485-203	1" RING	277
205	000-20485-204	1" RING	278
206	000-20485-205	1" RING	279
207	000-20485-206	1" RING	280
208	000-20485-207	1" RING	281
209	000-20485-208	1" RING	282
210	000-20485-209	1" RING	283
211	000-20485-210	1" RING	284
212	000-20485-211	1" RING	285
213	000-20485-212	1" RING	286
214	000-20485-213	1" RING	287
215	000-20485-214	1" RING	288
216	000-20485-215	1" RING	289
217	000-20485-216	1" RING	290
218	000-20485-217	1" RING	291
219	000-20485-218	1" RING	292
220	000-20485-219	1" RING	293
221	000-20485-220	1" RING	294
222	000-20485-221	1" RING	295
223	000-20485-222	1" RING	296
224	000-20485-223	1" RING	297
225	000-20485-224	1" RING	298
226	000-20485-225	1" RING	299
227	000-20485-226	1" RING	300
228	000-20485-227	1" RING	301
229	000-20485-228	1" RING	302
230	000-20485-229	1" RING	303
231	000-20485-230	1" RING	304
232	000-20485-231	1" RING	305
233	000-20485-232	1" RING	306
234	000-20485-233	1" RING	307
235	000-20485-234	1" RING	308
236	000-20485-235	1" RING	309
237	000-20485-236	1" RING	310
238	000-20485-237	1" RING	311
239	000-20485-238	1" RING	312
240	000-20485-239	1" RING	313
241	000-20485-240	1" RING	314
242	000-20485-241	1" RING	315
243	000-20485-242	1" RING	316
244	000-20485-243	1" RING	317
245	000-20485-244	1" RING	318
246	000-20485-245	1" RING	319
247	000-20485-246	1" RING	320
248	000-20485-247	1" RING	321
249	000-20485-248	1" RING	322
250	000-20485-249	1" RING	323
251	000-20485-250	1" RING	324
252	000-20485-251	1" RING	325
253	000-20485-252	1" RING	326
254	000-20485-253	1" RING	327
255	000-20485-254	1" RING	328
256	000-20485-255	1" RING	329
257	000-20485-256	1" RING	330
258	000-20485-257	1" RING	331
259	000-20485-258	1" RING	332
260	000-20485-259	1" RING	333
261	000-20485-260	1" RING	334
262	000-20485-261	1" RING	335
263	000-20485-262	1" RING	336
264	000-20485-263	1" RING	337
265	000-20485-264	1" RING	338
266	000-20485-265	1" RING	339
267	000-20485-266	1" RING	340
268	000-20485-267	1" RING	341
269	000-20485-268		



are in agreement.

Majority operation is possible because of the ability of the armature of the torque motor to be essentially a free beam sensitive to force balances. For instance, if one torque motor should receive a hardover command, then its torque motor would be satisfied only when a hardover feedback to the torque motor existed. However, the remaining two torque motors would be satisfied when the feedback torque equalled their input torque, which for this example we can say is zero (actuator centered). The action that would take place for this example is as follows: (1) The flapper of the hardover torque motor would seal against one nozzle of its hydraulic amplifier, (2) the flappers of the remaining two torque motors would seek a position such that equal hydraulic pressures would continue to exist at the second stage spool end chambers, (3) the servovalve would remain at null and the actuator centered. The hardover torque of the failed motor would be balanced by the mechanical torque produced at the sealed nozzle. The zero torque input of the remaining two (or majority of the) motors would be satisfied by the actuator centered position. Similar analogies can be made for the cases of nozzle plugging, fail neutral, plugged inlet orifice, and partial failure of any one first stage torque motor hydraulic amplifier assembly. The majority voting servovalve will also vote if a failure occurs in one of the connecting cables of the servoamplifiers.

The method of providing DPF consists of an auxiliary pair of nozzles to each torque motor, together with two spring centered pistons. Load pressures are applied to either end of the nozzle on one side of each torque motor flapper. The nozzle-flapper acts as a resistance that is sensitive to flow; that is, its resistance increases with increased flow. The spring centered pistons act as capacitances which are coupled with the nozzle-flappers to form a frequency sensitive network.

Static or very low frequency load pressure changes result in displacement of the auxiliary pistons against their springs. As the frequency of load pressure change is increased, the fluid of the annular sections of the pistons must attempt to pass by the nozzle-flappers at ever increasing rates. Because the nozzle-flapper resistance is sensitive to flow, at higher frequencies the resistance increases and pressures proportional to load

pressures (by the area ratio of the auxiliary pistons) are imposed on the flapper. These dynamic load pressures produce a torque on each flapper. Servovalve performance is thus modulated by this action and feedback polarity is arranged so as to produce damping. As was the case for basic servovalve operation, three sets of auxiliary nozzles are utilized in order to retain majority voting capability. The use of two spring centered pistons provides redundancy in that if one piston fails (seizure or broken spring), the DPF feature will be retained. In this case, the frequency at which load damping becomes effective will increase. Sizing is such that damping takes place well below the resonant frequency.

Additional auxiliary features are provided in the servoactuator. Items included are a prefiltration valve, a cylinder bypass valve (manual and hydraulically operated) and a strain gage telemetering device. Ground support items include a removable mid-stroke lock and a position indicator scale and vernier.

### 3.3 Design Features

The actuator design is based upon the present 17-189 (S-IV B) actuator. An aluminum alloy barrel is used with a high expansion steel alloy piston. In order to maintain the present S-IV B end fitting, it was necessary to reduce the stroke of the actuator from approximately  $\pm 1 \frac{1}{2}$  inches to  $\pm 1 \frac{1}{4}$  inches. The reduction in stroke was caused by the valve configuration. The majority voting servovalve maintained the rugged straightforward design of the present S-IV B valve. The basic fundamental that was followed in the servovalve design was to not compromise reliability in order to package added components. Just as in the S-IV B servovalve, there are no levers, links or gimmicks used in the feedback mechanism. However, a price must be paid for this type of straightforward design, and that price is added actuator length or reduced actuator stroke. Since the actuator length was fixed and there is good reason to assume that the actuator stroke could be reduced, the latter course was taken.

The valve is a modular design. It consists of three separable first stage torque motor assemblies, a second stage spool-bushing assembly, and a cam, cam housing assembly mounted to a stainless steel valve body. The first stage torque motor assemblies have

been made as identical to one another as possible, to minimize the differences in thermal, dynamic, and vibrational characteristics. Two of the first stage assemblies utilize the balanced armature feedback concept of the S-IV B valve; the third first stage utilizes the extended flapper feedback necessitated by the design limitations discussed in the previous paragraph.

The first stage torque motor assemblies contain the torque motor, flapper and first stage nozzles, first stage filter orifice assembly, DPF nozzles, and individual DPF nozzle filters.

The second stage spool bushing design is straightforward. The bushing is flange mounted and has a laminar fit into a dead ended bore. The flange mounted bushing is employed to compactly package the cam, cam housing assembly at the opposite end of the valve body. The amplifier passages from the first stage nozzles terminate in common chambers at the ends of the spool. The DPF nozzles are joined in a common annular bushing groove and ported out through the base of the valve to the DPF pistons.

The cam and cam housing mount into a lap fit hole in the valve body. The cam housing is restrained from rotational motion by a keyway and from translational motion by a tie-wired nut. The three leaf spring followers attach to the cam housing. These followers are the same as those used on the S-IV B valve. However, the leaf spring used on the flapper extension feedback assembly is made of a non-magnetic material because it operates in close proximity to the air gap of the torque motor.

The DPF pistons for the servovalve are located in the actuator. This is the same arrangement used on the S-II and the S-IV B actuators. Two DPF pistons are used to provide redundancy. Only two pistons are required to provide redundant operation because their mode of failure is passive.

Redundant connectors are provided for the servovalve in order to maintain the majority voting concept all the way to the servo-actuator input.

Telemetry information on actuator position is accomplished by strain gage elements mounted on two of the cantilever beam cam follower arms. This method of obtaining actuator piston information has been developed by Moog to eliminate the telemetry



potentiometer. Tests conducted on these devices indicate that they are as good or better than potentiometers and they add no extra weight. More importantly, the use of the strain gage elements eliminates the reliability compromise of driving the feedback cam with the shaft of the telemetry pot.

The prefiltration valve and the cylinder bypass valve are of a modular design identical to those now being used in the S-IV B. The actuator drawing indicates provisions for mounting the same customer supplied equipment; i.e., temperature transducer and differential pressure transducer, as the S-IV B.

The mid-position lock and the position indicator are similar in design to those now used on the S-IV B. They have been modified to take advantage of the shorter actuator stroke.

The actuator materials are stainless steel, anodized aluminum, cadmium plated steel, and titanium. Their usage is the same as in the present S-IV B actuator.

The weight of the majority voting actuator is 46 pounds compared to the present S-IV B actuator weight of 40 pounds.

The design of the actuator is characterized by rugged straight-forward construction. The ultimate goal was the highest possible unit reliability. Where compromises had to be made they were made at the expense of stroke, weight or envelope.

#### 4.0 TEST RESULTS

Assembly of the servoactuator presented no gross problems. Minor mechanical type problems requiring some dimensional changes to detail parts were encountered, but this is typical of first hardware in any development program. During set-up of the servovalve, magnetic interaction of the torque motors due to their proximity to each other was observed and caused some problem. Recognition of the problem led to suitable set-up techniques which negated the interaction.

Views of a completed actuator are given in Fig. 1 and 2. An exploded view is given in Fig. 3. The servovalve assembly and partial views of the servovalve are given in Figures 4, 5, and 6.

The servoactuators successfully met all performance goals. These goals were to perform within the S-IV B requirements, with and without failures in a single channel, and to exhibit less than 5% shift in actuator position following a failure.

The expected performance was indicated by Moog Report ER-88. This report indicated expected performance at a position loop gain,  $K_{vx}$ , of  $20 \text{ sec}^{-1}$ , and a dynamic pressure loop gain,  $K_{vp}$ , of  $33.2 \text{ sec}^{-1}$  and presented the sizing calculations used in establishing the gain values. The servovalves for the program were initially built to the values specified in ER-88. However, as a result of the development testing of the S-IV B system, it became apparent that system resonance was at a lower frequency than that originally calculated. Original system resonance had been stated as  $57.1 \text{ rad/sec}$ , and the later value was  $43.0 \text{ rad/sec}$ . Production S-IV B actuator gains were adjusted in order to provide acceptable system performance. Discussions between NASA (M. Kalange) and Moog Engineering (W. J. Thayer) in November of 1964 resulted in agreement to change the S-IV B majority voting actuator to have identical gains to that of the production S-IV B. Revision ER-88A reflected the necessary sizing changes and indicated expected performance. Moog reports ER-88 and ER-88A are included in the appendix of this report. A nominal position loop gain,  $K_{vx}$ , of  $14.25 \text{ sec}^{-1}$  and a dynamic pressure loop gain of  $20.4 \text{ sec}^{-1}$  is indicated in ER-88A. The actuators built under this program had gain values as follows:

	$K_{vx}$	$K_{vp}$
Actuator S/N 1	$16.1 \text{ sec}^{-1}$	$17.6 \text{ sec}^{-1}$
Actuator S/N 2	$15.8 \text{ sec}^{-1}$	$20.2 \text{ sec}^{-1}$

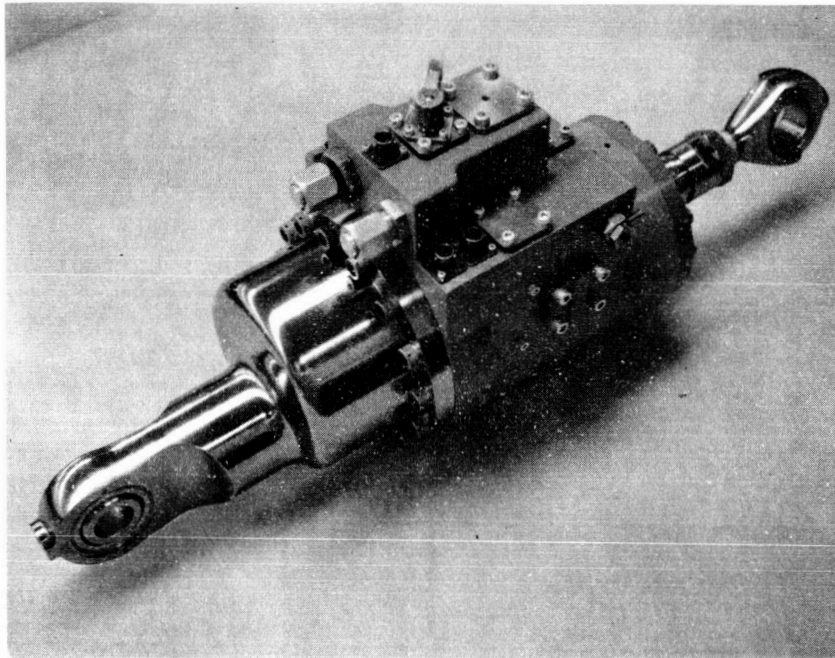


Fig. 1 Completed S-IV B  
Majority Voting Actuator

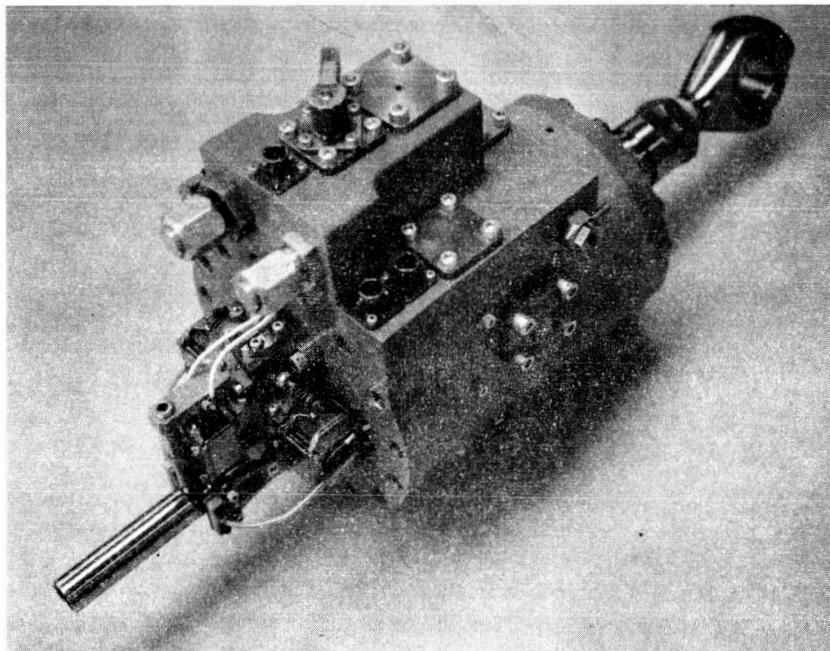


Fig. 2 Completed S-IV B Majority Voting  
Actuator with Tailstock Removed

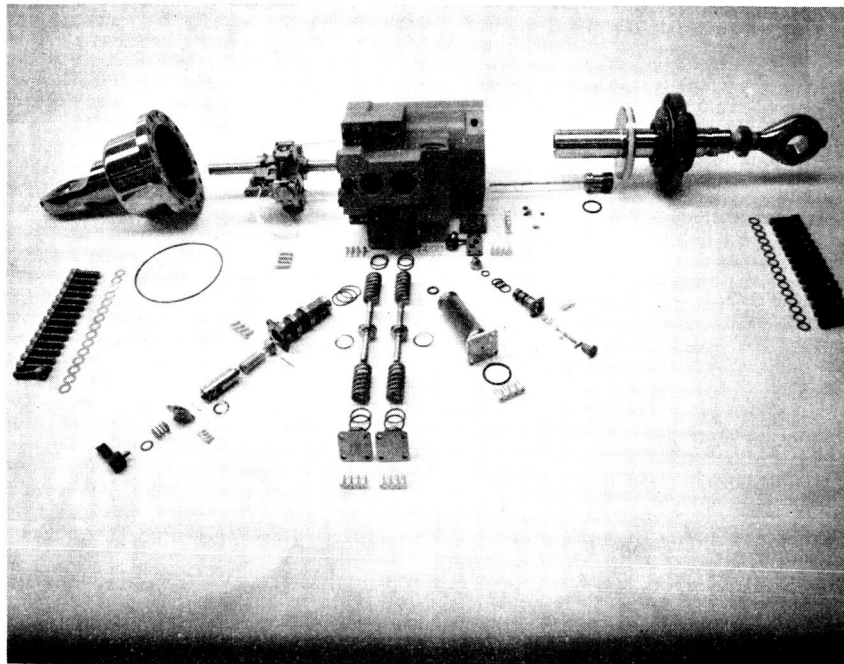


Fig. 3 Exploded View of S-IV B  
Majority Voting Actuator

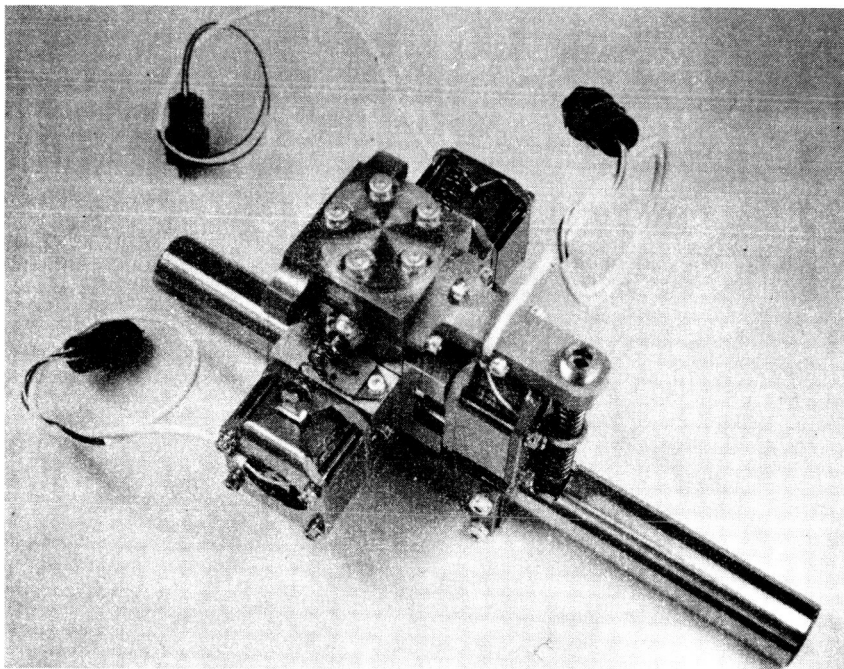


Fig. 4 Majority Voting Valve, Cam  
Housing, and Cam Assembly

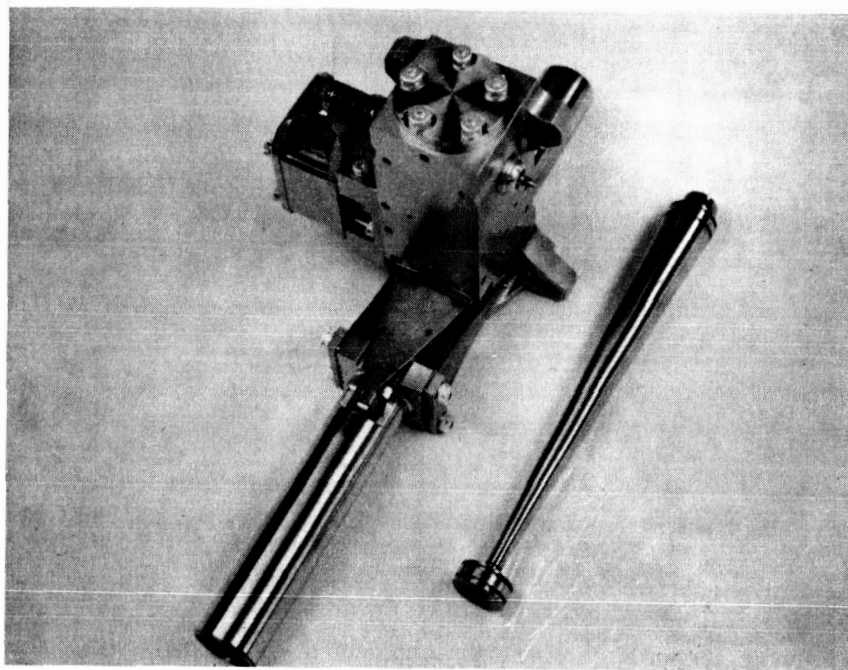


Fig. 5 Partial Assembly: Valve, Cam Housing, and Cam

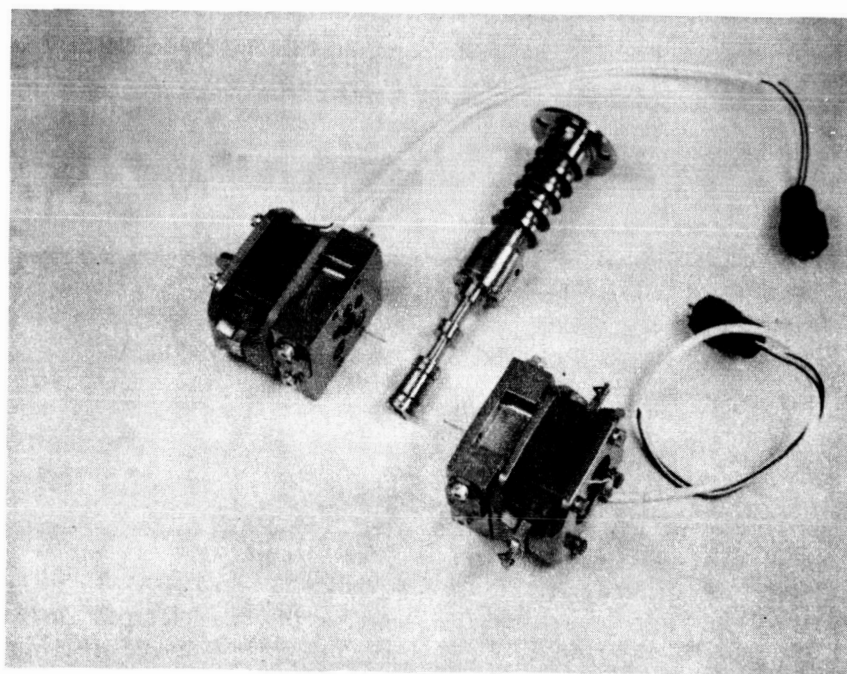


Fig. 6 Detail Parts: Torque Motor Assemblies and Valve Spool - Bushing Assembly

The following pages contain data typical of the two actuators. All data is from Actuator S/N 2.

Figure 7 is a plot of actuator position vs. input signal with all channels active. Relationships such as midstroke lock to extend and retract positions, and mid-stroke lock to telemetry strain gage zero are also given on this plot. Note that the indicated position (as given by strain gage output) and actual actuator position differ by one and one-half percent from mid-stroke to either full extend or full retract due to the non-linearity of the strain gage output. Figures 8, 9, and 10 indicate the output characteristics of the actuator with open and hard-over failures in each of the three channels. Figures 11, 12, and 13 are plots taken under the same conditions, but having each plot run with its own axis rather than a common axis in order that a more accurate assessment can be made of actuator change in position following the introduction of a simulated failure. Maximum shift observed was 4% (see Fig. 13).

Dynamic characteristics of the servoactuator with and without simulated failures were also assessed. The servovalve's open loop dynamic characteristics under conditions of no failure, hard-over failure of one torque motor, or open (coil) failure of one torque motor are given in Figures 14 thru 19. These figures indicate dynamic characteristics for the case of failure of the three motors, one at a time, and also reflect the effect of input amplitude. Figures 20 and 21 are plots of dynamic characteristics taken on the S-IV B load simulator at two different command amplitudes to the servoactuator. From the plots it can be seen that the dynamic characteristics remain essentially unchanged following an induced failure in one channel. Comparison of the actual data with the expected performance predicted in ER-88A indicates that phase lag is less than predicted and the amplitude ratio has a higher peak value than predicted. A portion of this discrepancy can be attributed to the fact that the actual loop gain of the servoactuator was somewhat higher than nominal gain ( $15.8 \text{ sec}^{-1}$  vs.  $14.25 \text{ sec}^{-1}$ ), but it is also true that greater peak amplitude is generally seen on actual test due to mechanical characteristics of the actuator and load simulator, such as back-lash of bearings.

Step input tests at various command inputs and with simulated failures were also conducted on the load simulator. Observed characteristics are illustrated by the photographs of Figures 22 thru 27. Again, it can be observed that transient response remains essentially unchanged following an induced failure in one channel.



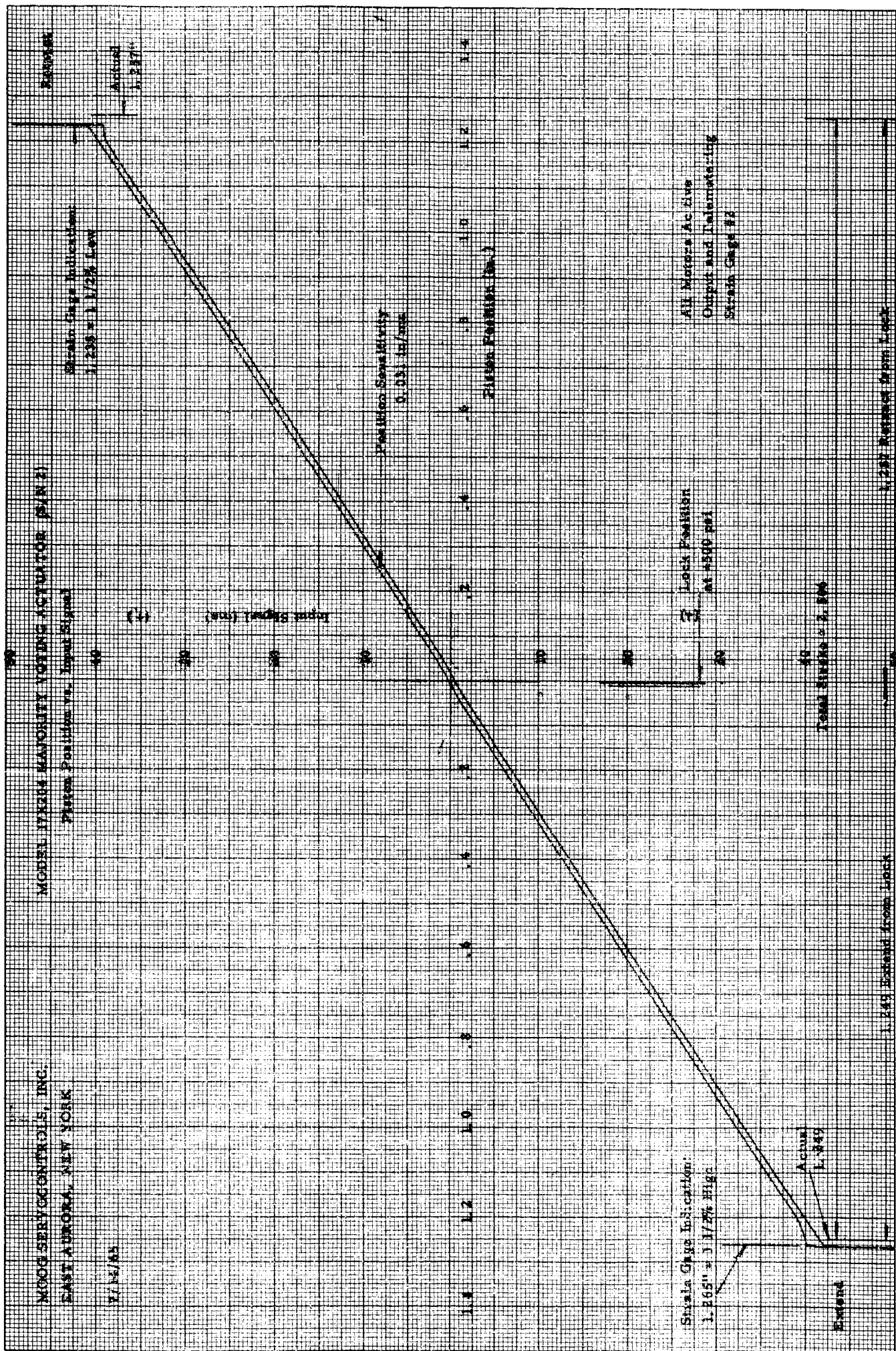


Fig. 7

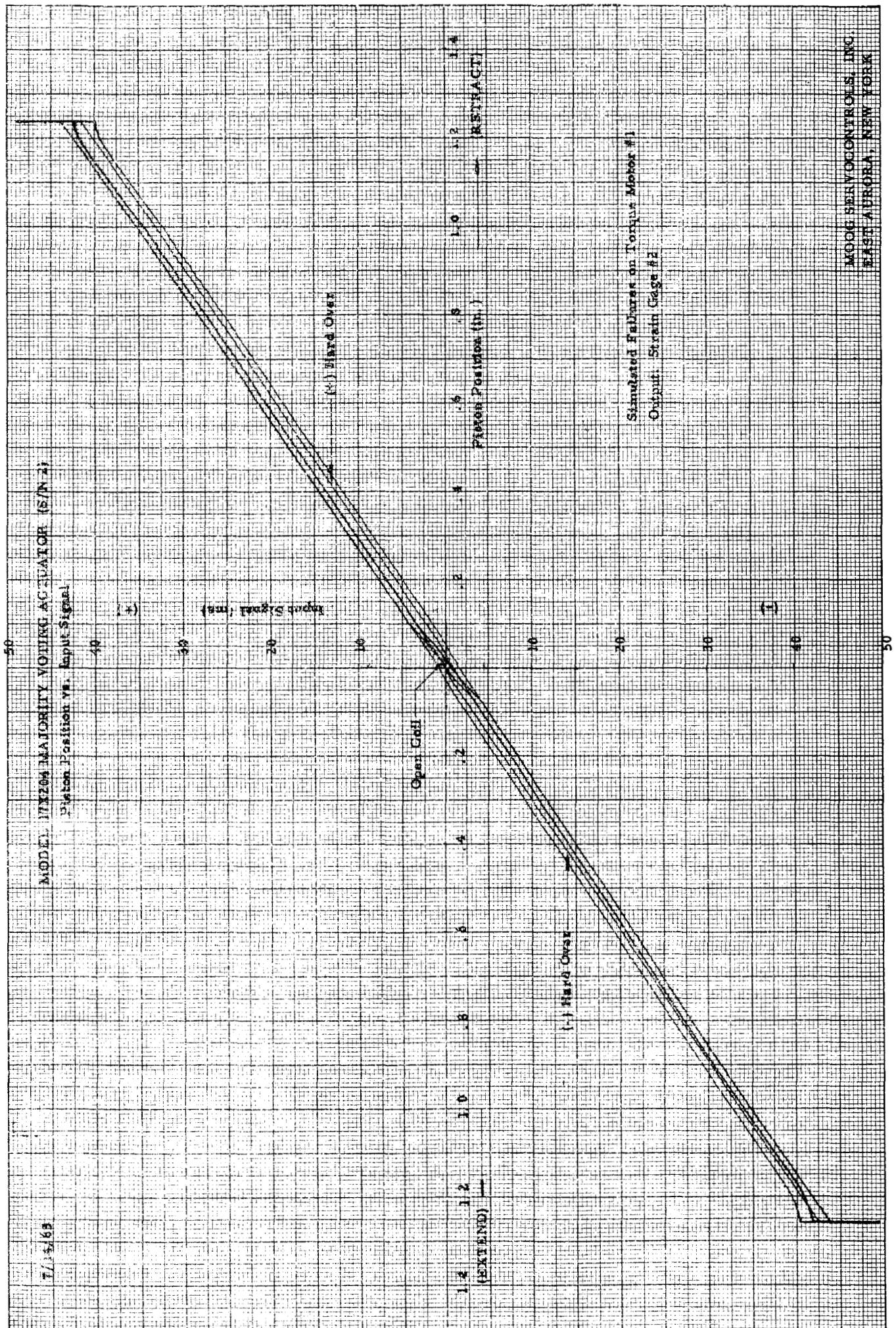


Fig. 8



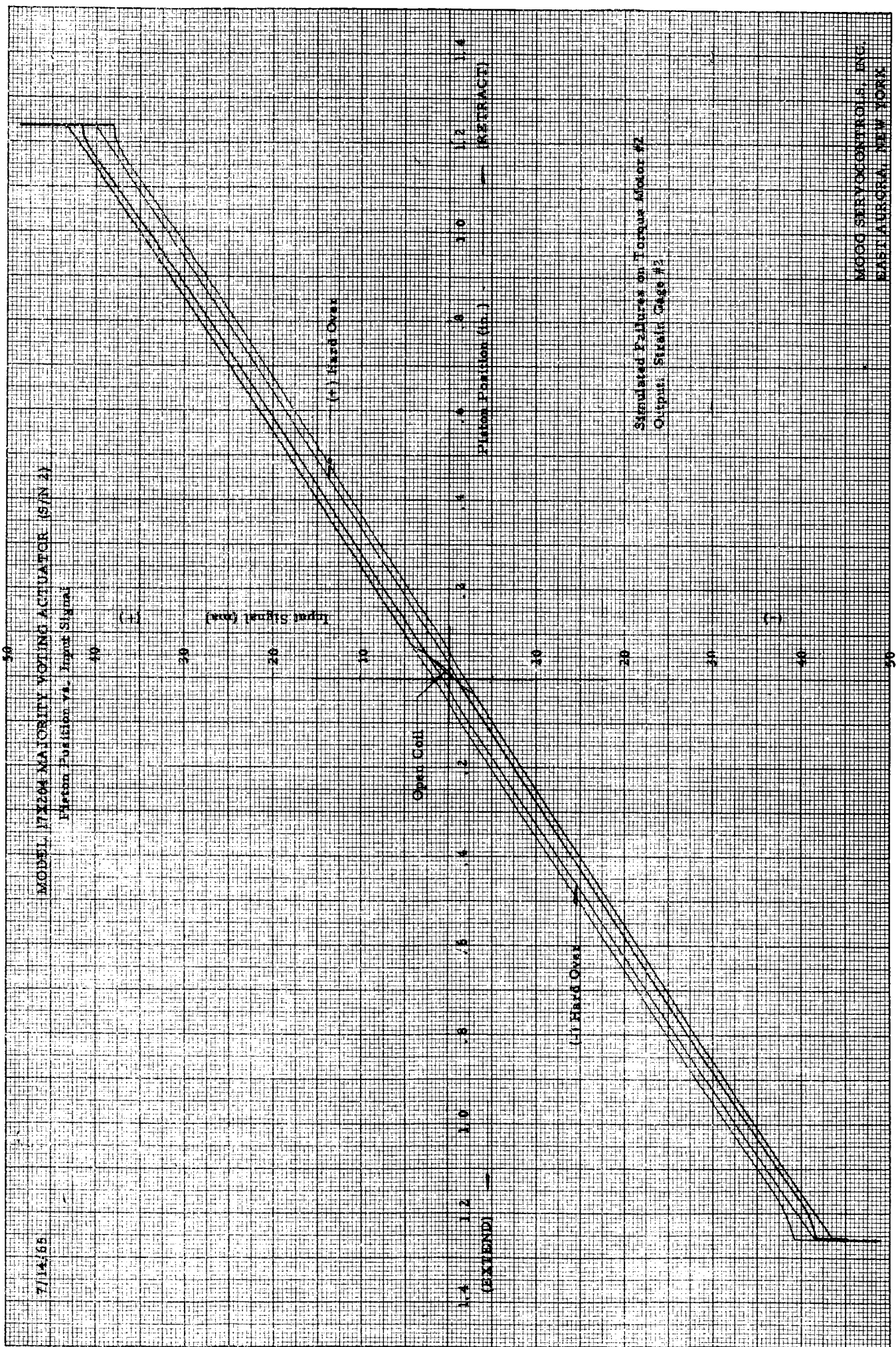


Fig. 9

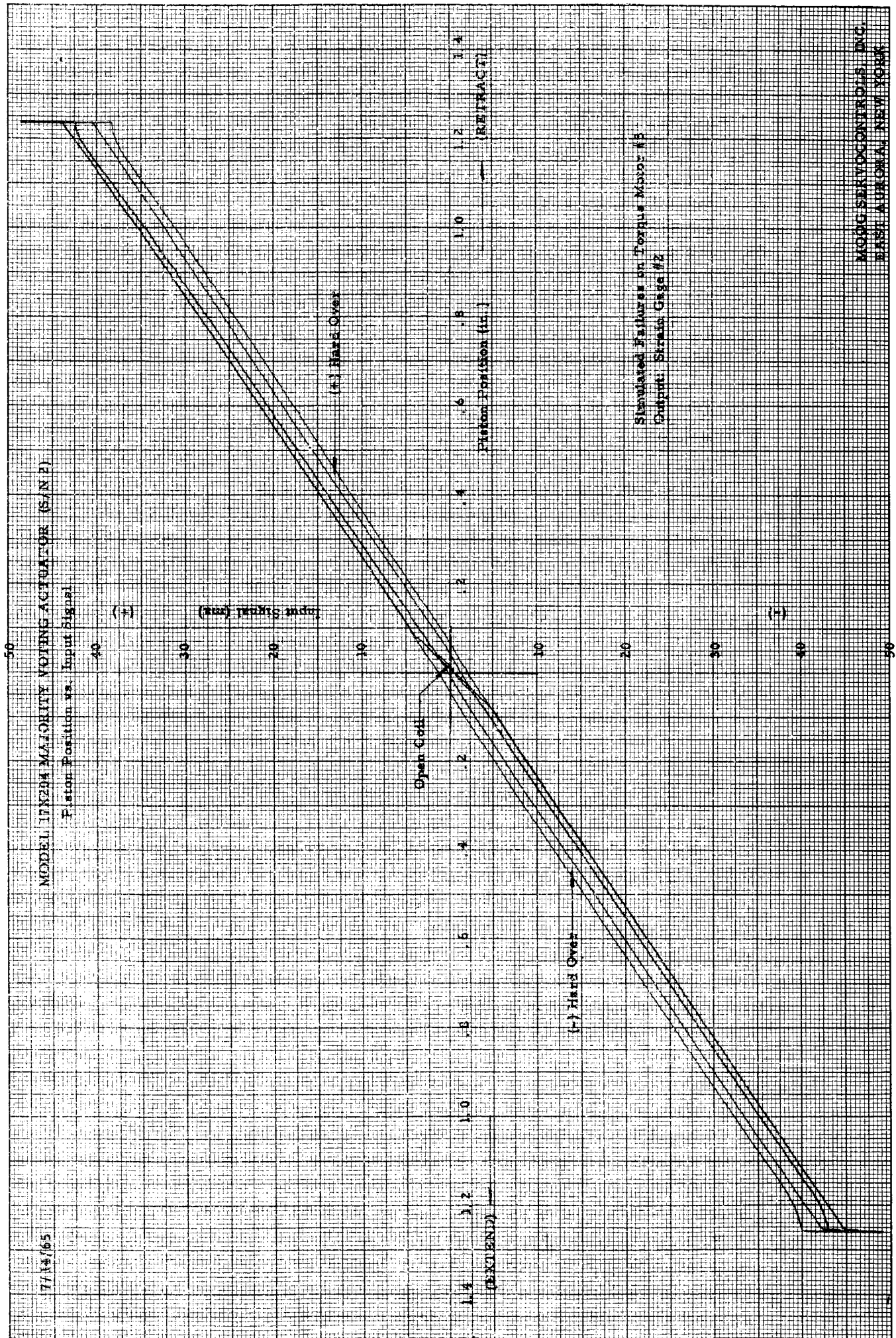


Fig. 10



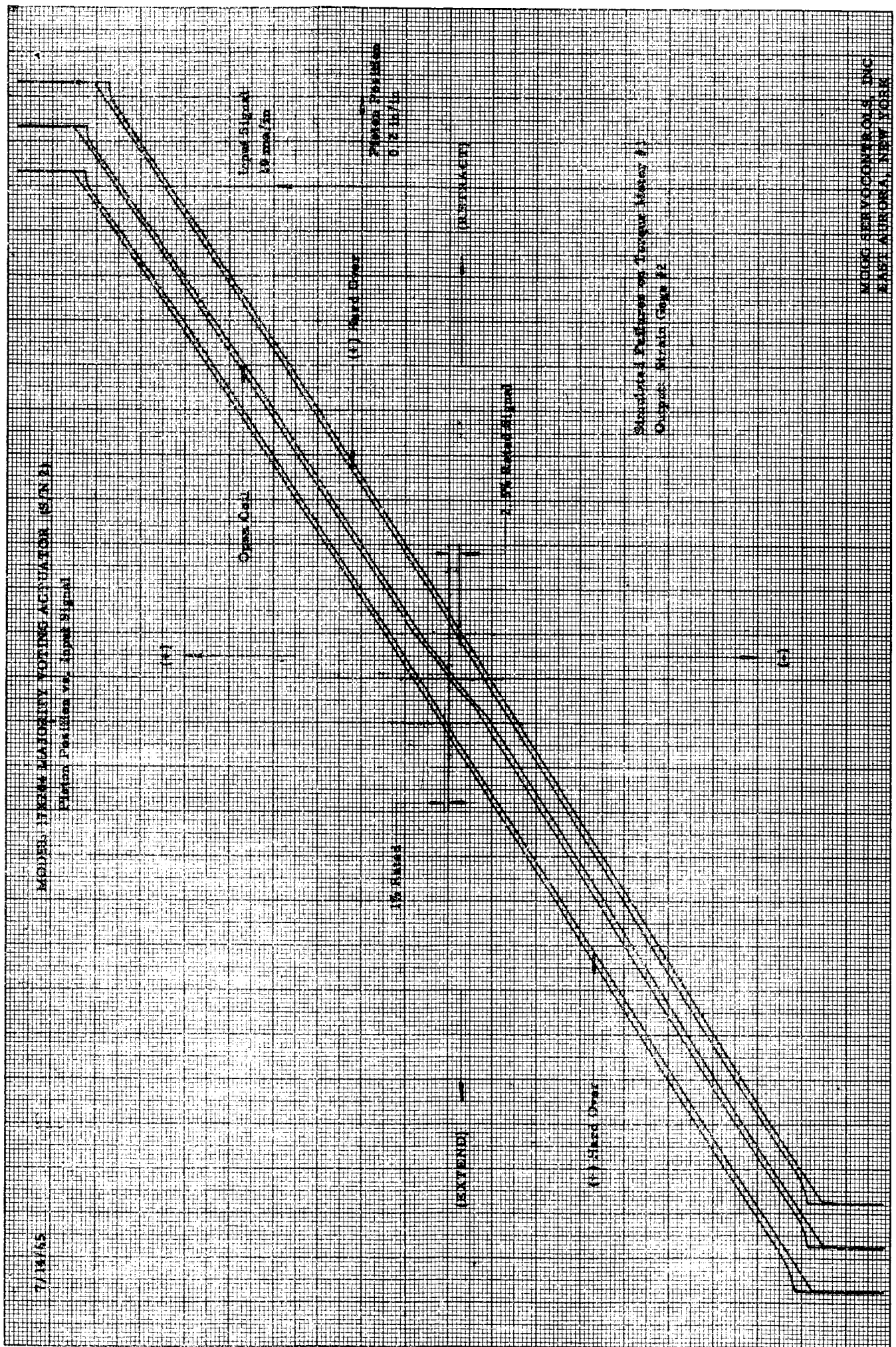
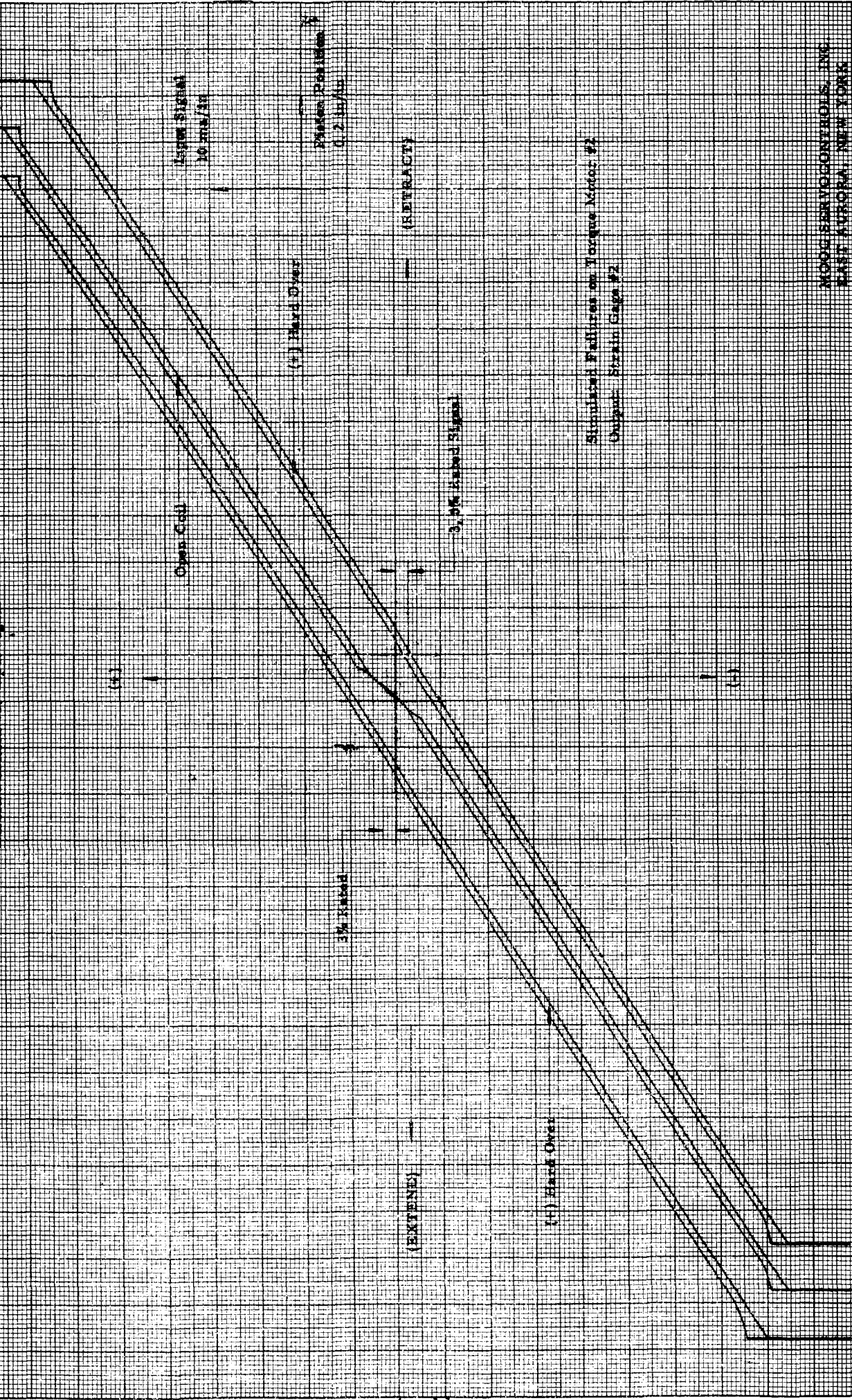


Fig. 11

7/14/53

# MODEL 17204 MAJORITY VOTING ACTUATOR (SIN 2)

Piston Position vs. Input Signal



Simulated Failures on Torque Motor #2  
Output: Strain Gage #2

MOOG SERVO CONTROLS, INC.  
EAST AURORA, NEW YORK

Fig. 12



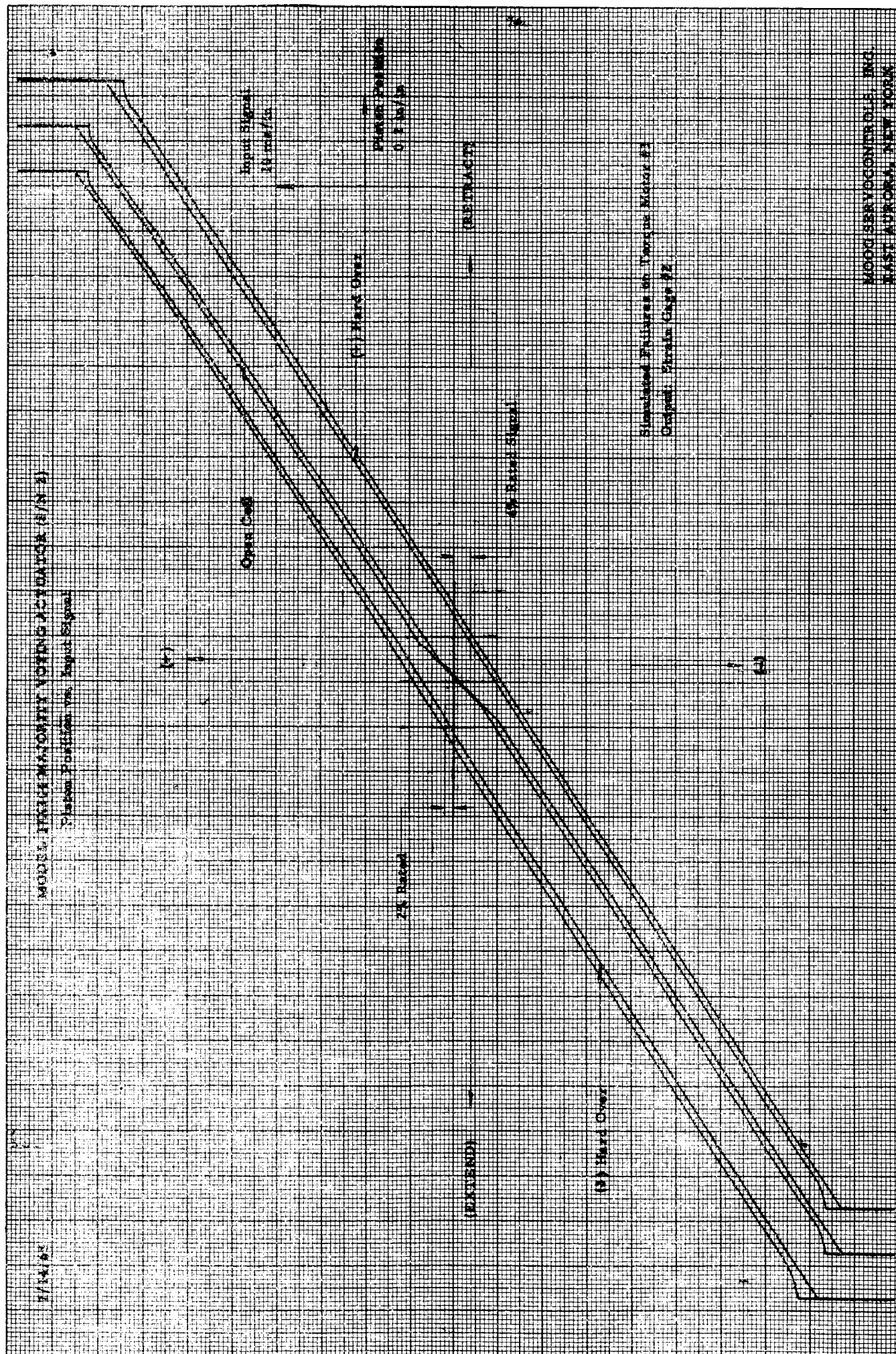
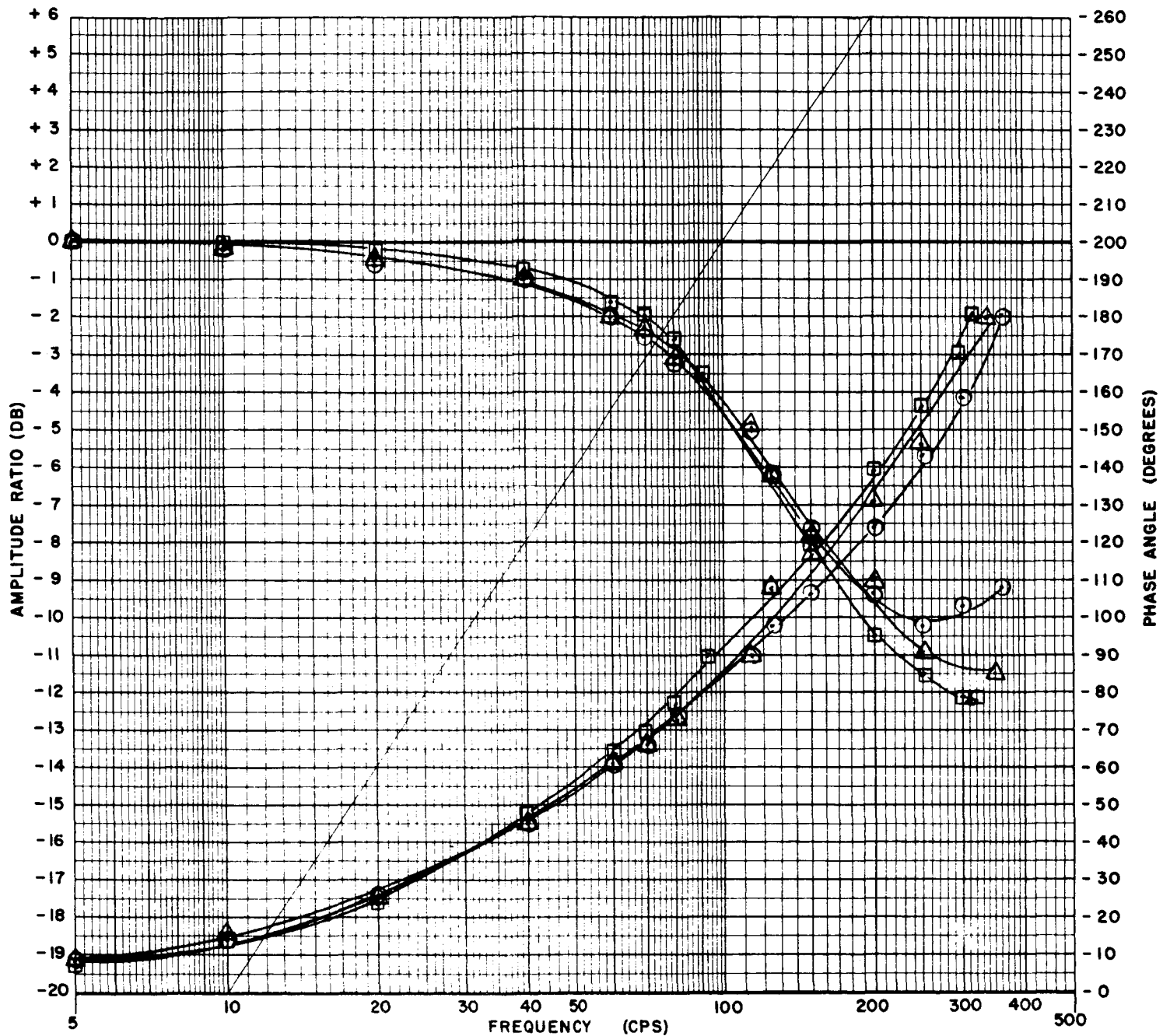


Fig. 13

# SERVO VALVE DYNAMIC RESPONSE



MODEL 16-147 SERIAL 3

DATE 6-2-65 BY lh

SYSTEM PRESSURE 3500 PSI

INPUT SIGNAL 1 MA.(P-P)

OUTPUT No Load Flow

Torque Motor #1 Failed

**MOOG SERVOCONTROLS, INC.**

EAST AURORA, NEW YORK

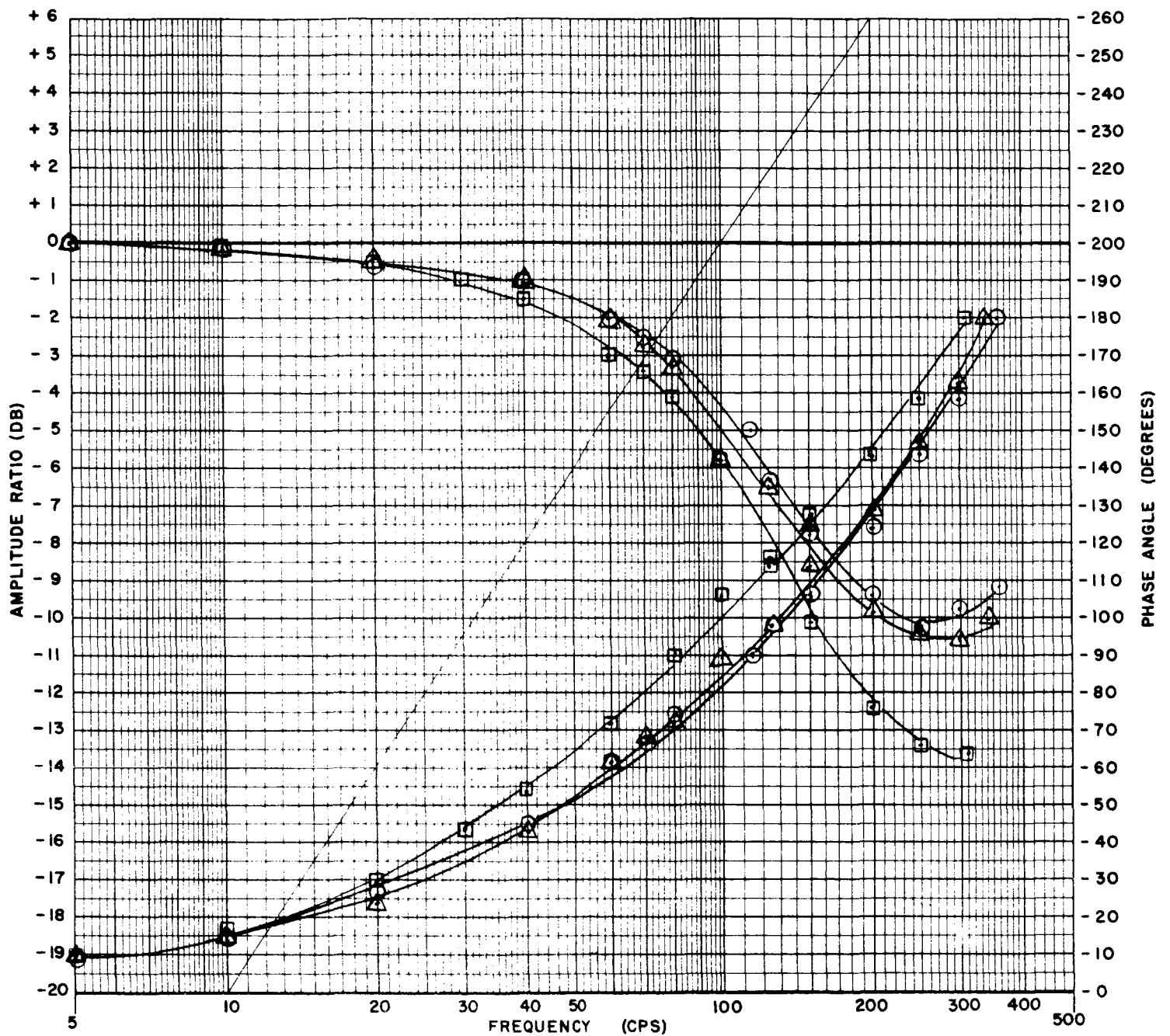
Fig. 14

○ - No Failure

△ - Open

□ - +50 ma

# SERVO VALVE DYNAMIC RESPONSE



MODEL 16-147 SERIAL 3

DATE 6-2-65 BY lh

SYSTEM PRESSURE 3500 PSI

INPUT SIGNAL 1 MA.(P-P)

OUTPUT No Load Flow

Torque Motor #2 Failed

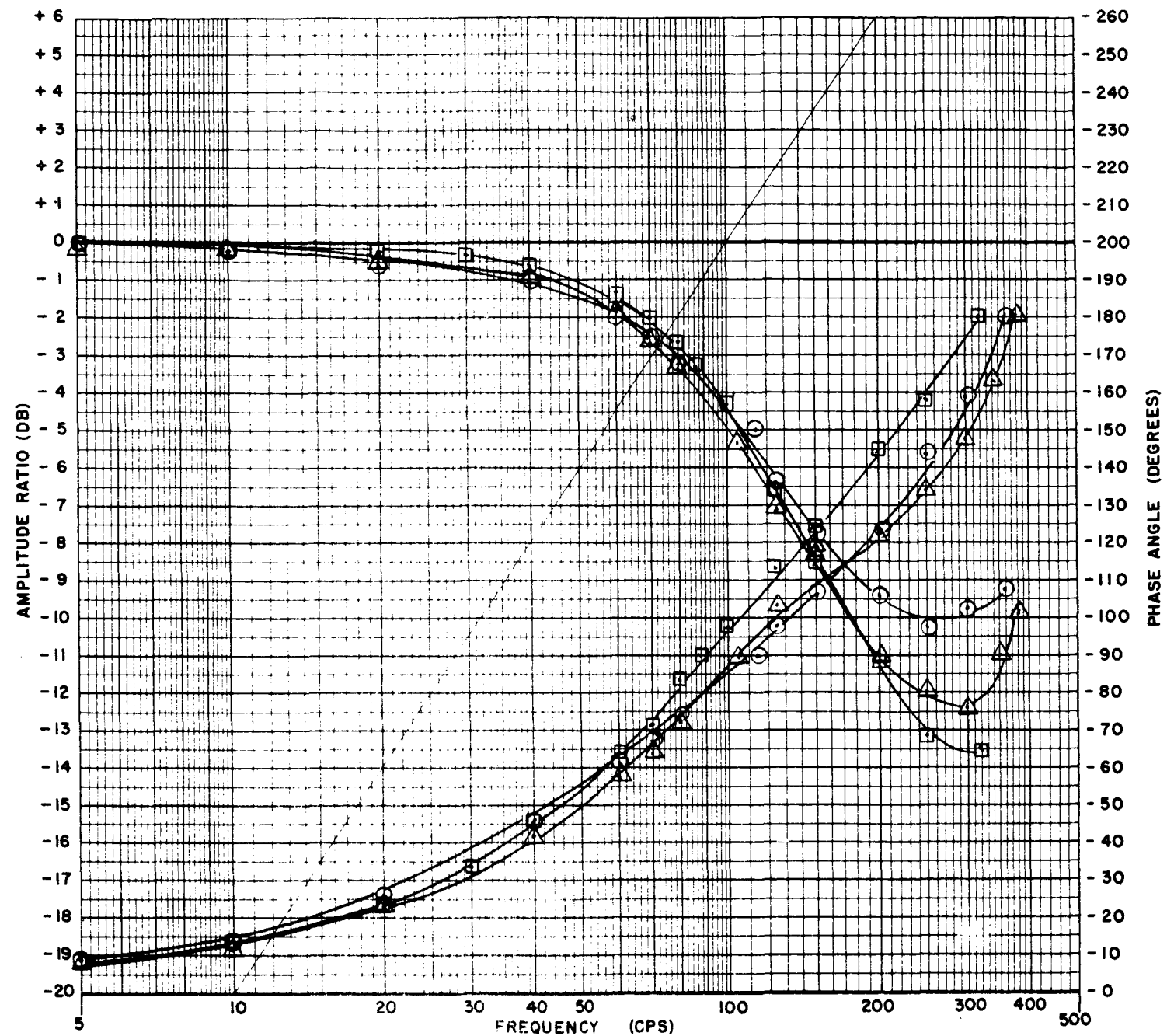
**MOOG SERVOCONTROLS, INC.**  
EAST AURORA, NEW YORK

Fig. 15 ○ - No Failure

△ - Open

□ - +50 ma

# SERVO VALVE DYNAMIC RESPONSE



MODEL 16-147 SERIAL 3

DATE 6-2-65 BY lh

SYSTEM PRESSURE 3500 PSI

INPUT SIGNAL 1 MA.(P-P)

OUTPUT No Load Flow

Torque Motor #3 Failed

**MOOG SERVOCONTROLS, INC.**  
EAST AURORA, NEW YORK

Fig. 16

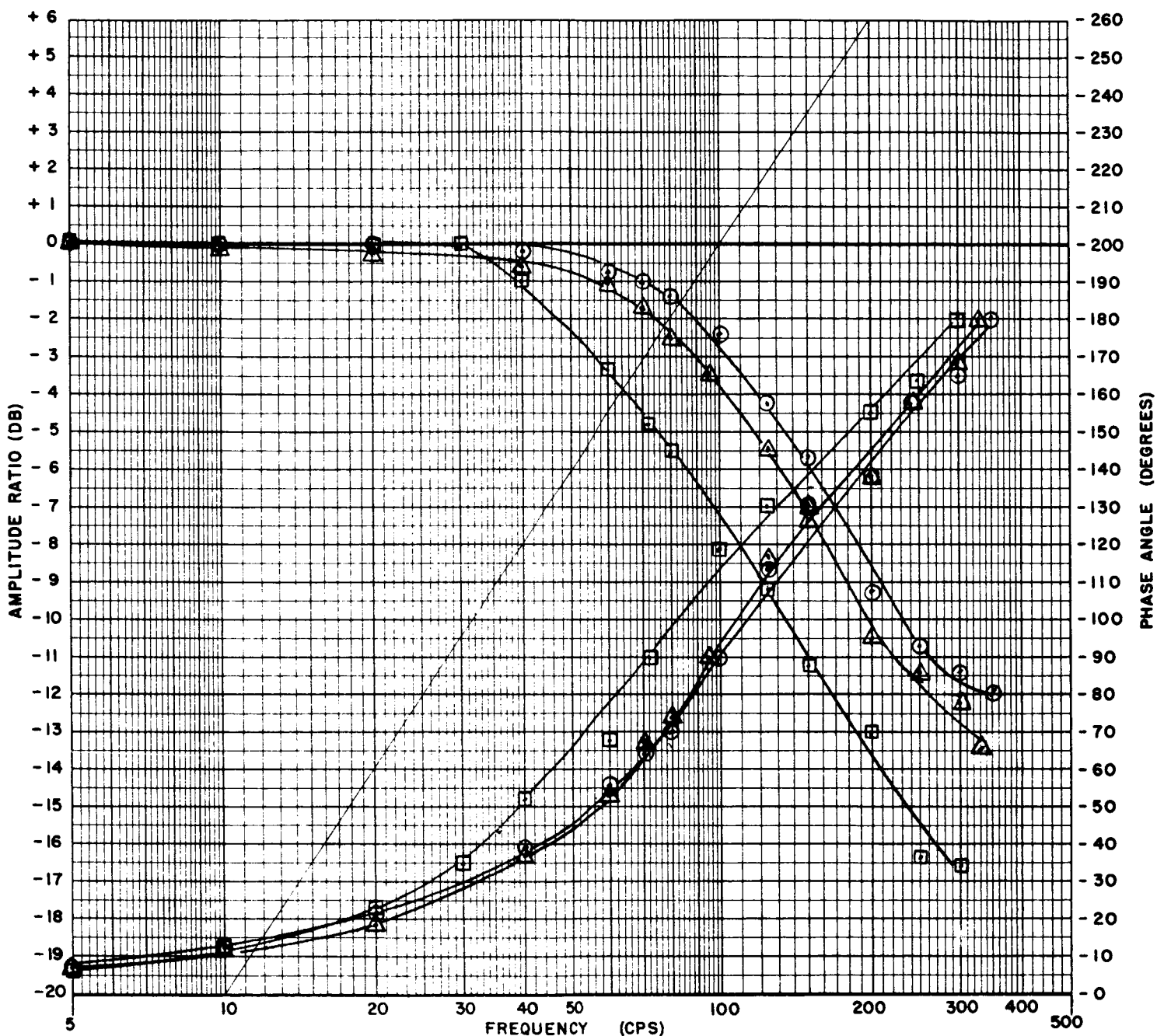
○ - No Failure

△ - Open

□ - +50 ma



# SERVO VALVE DYNAMIC RESPONSE



MODEL 16-147 SERIAL 3

DATE 6-2-65 BY lh

SYSTEM PRESSURE 3500 PSI

INPUT SIGNAL 10 MA.(P-P)

OUTPUT No Load Flow

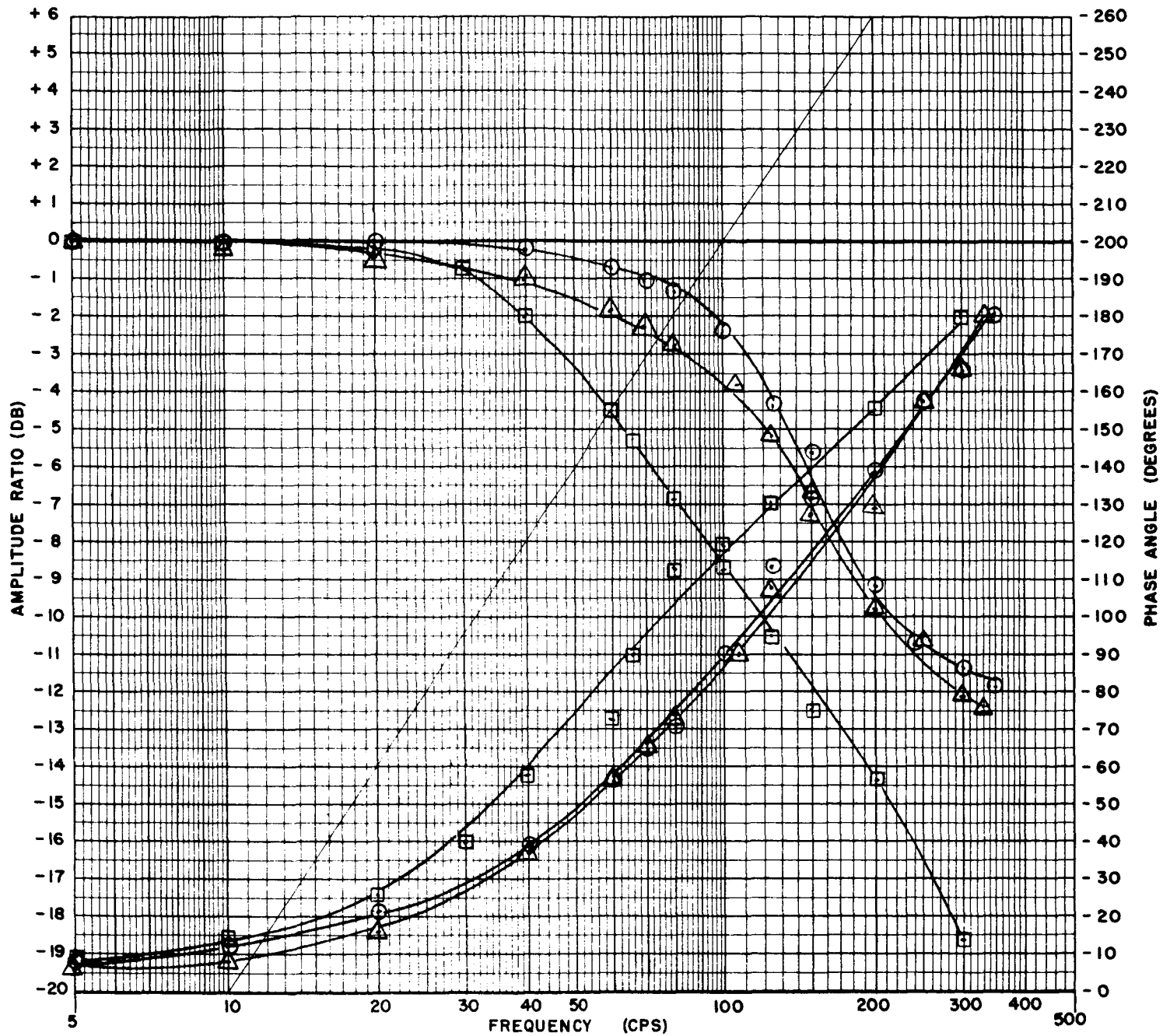
Torque Motor #1 Failed

**MOOG SERVOCONTROLS, INC.**  
EAST AURORA, NEW YORK

Fig. 17

- - No Failure
- △ - Open
- - +50 ma

# SERVO VALVE DYNAMIC RESPONSE



MODEL 16-147 SERIAL 3

DATE 6-2-65 BY lh

SYSTEM PRESSURE 3500 PSI

INPUT SIGNAL 10 MA.(P-P)

OUTPUT No Load Flow

Torque Motor #2 Failed

**MOOG SERVOCONTROLS, INC.**  
EAST AURORA, NEW YORK

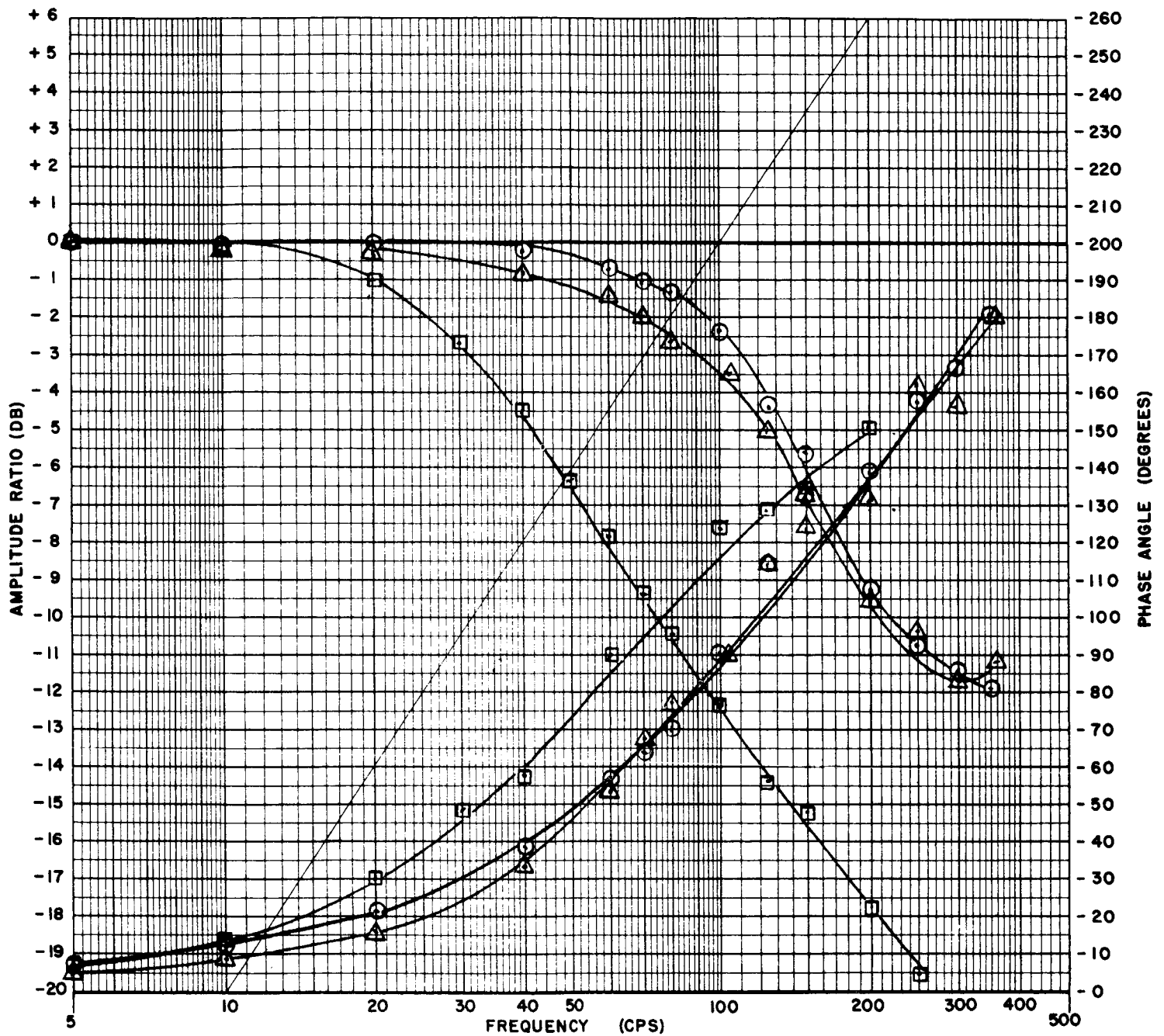
Fig. 18

○ - No Failure

△ - Open

□ - +50 ma

# SERVO VALVE DYNAMIC RESPONSE



MODEL 16-147 SERIAL 3

DATE 6-2-65 BY lh

SYSTEM PRESSURE 3500 PSI

INPUT SIGNAL 10 MA.(P-P)

OUTPUT No Load Flow

Torque Motor #3 Failed

**MOOG SERVOCONTROLS, INC.**  
EAST AURORA, NEW YORK

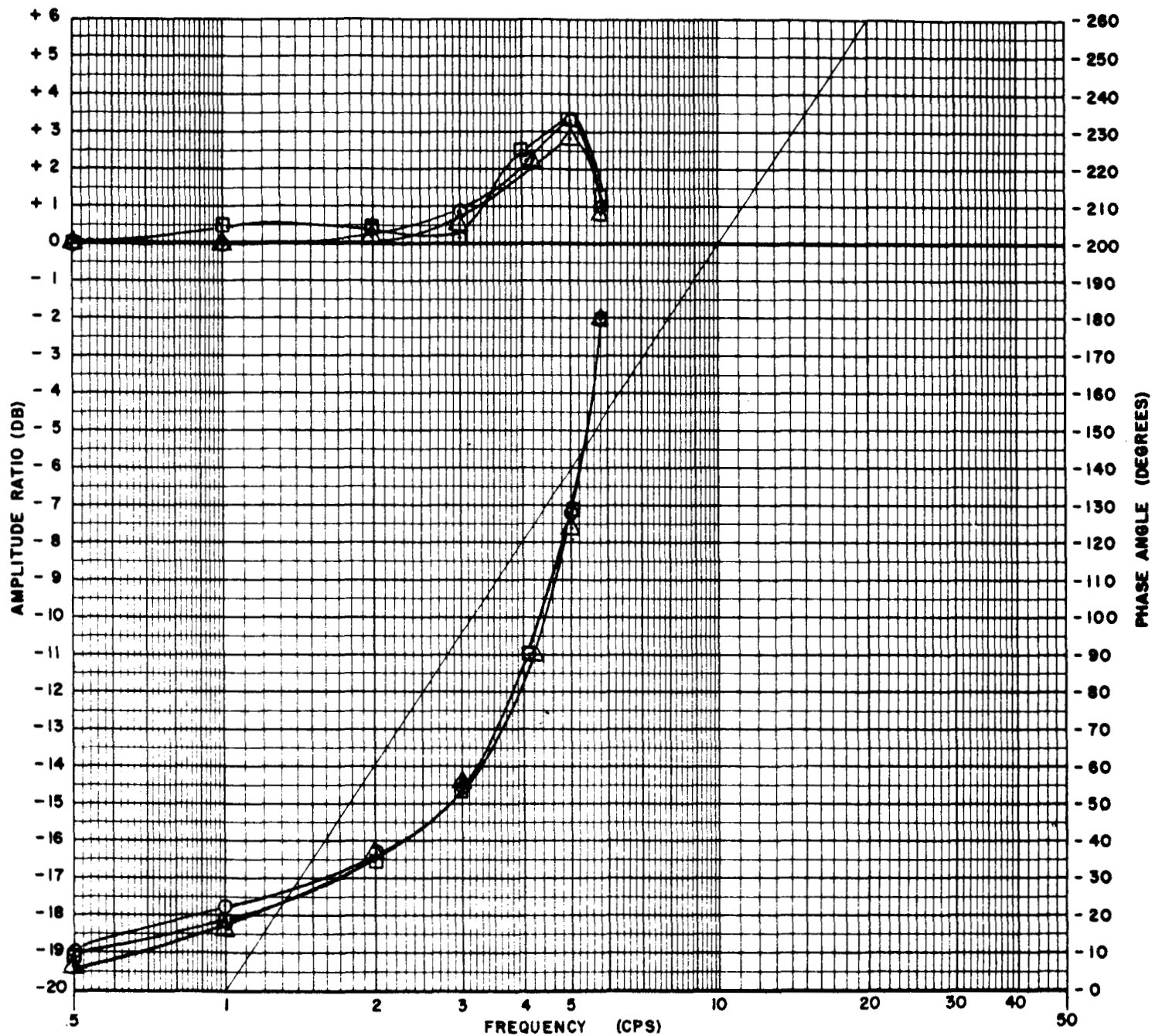
Fig. 19

○ - No Failure

△ - Open

□ - +50 ma

# SYSTEM RESPONSE



MODEL 17X204 SERIAL 2

DATE 6-17-65 BY lh

SYSTEM PRESSURE 3500 PSI

INPUT SIGNAL 3.5 MA.(P-P)

OUTPUT Simulator Load  
Position

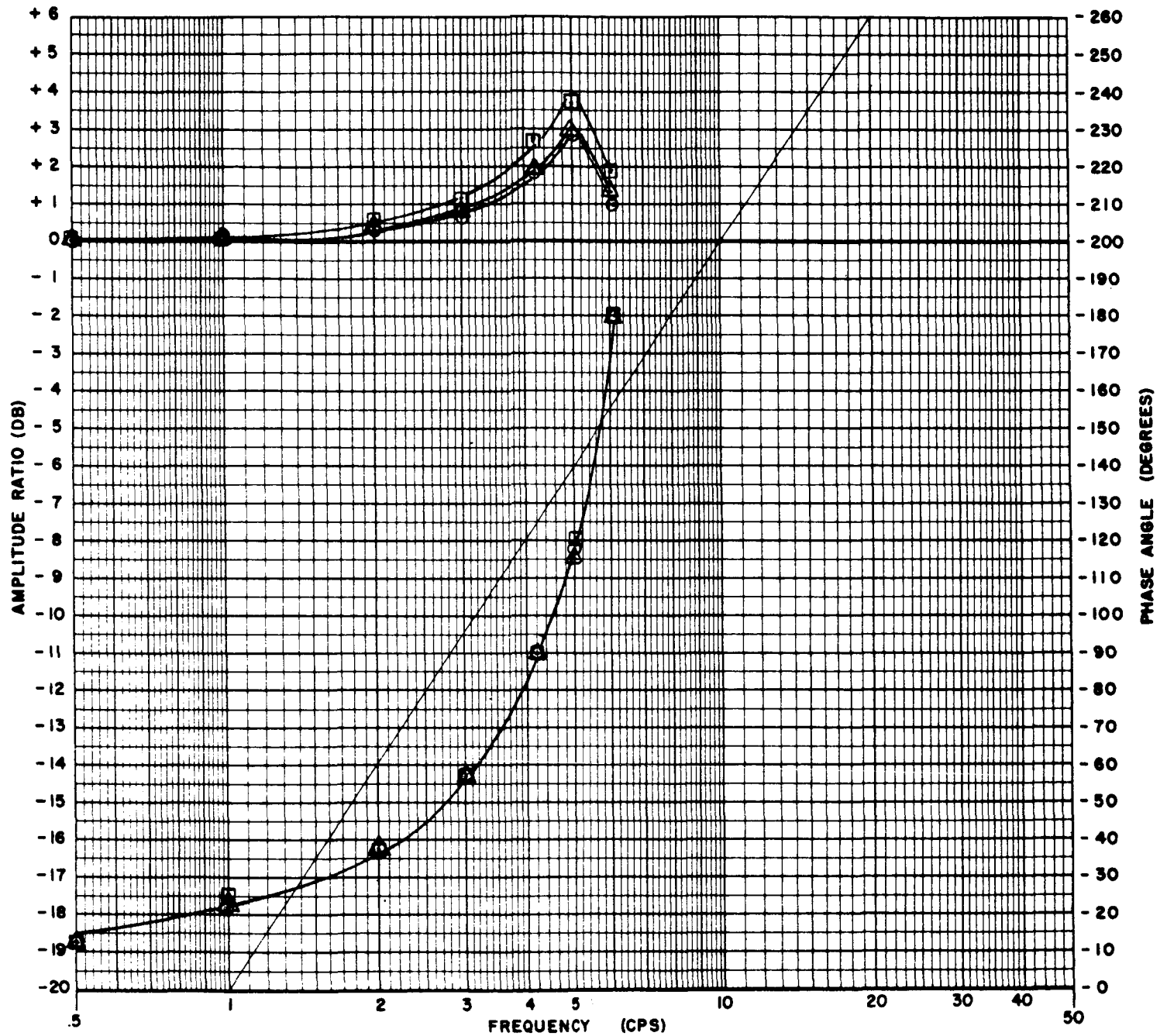
Fig. 20

4-19

**MOOG SERVOCONTROLS, INC.**  
EAST AURORA, NEW YORK

C

# SYSTEM RESPONSE



MODEL 17X204 SERIAL 2  
 DATE 6-17-65 BY lh

SYSTEM PRESSURE 3500 PSI  
 INPUT SIGNAL 7.0 MA.(P-P)  
 OUTPUT Simulator Load  
Position

○ - All Motors Active  
 $K_{vx} = 15.8 \text{ sec}^{-1}$

△ - (+) Hard Over } Torque Motor  
 □ - Open } #1 Failed

**MOOG SERVOCONTROLS, INC.**  
 EAST AURORA, NEW YORK

Fig.21

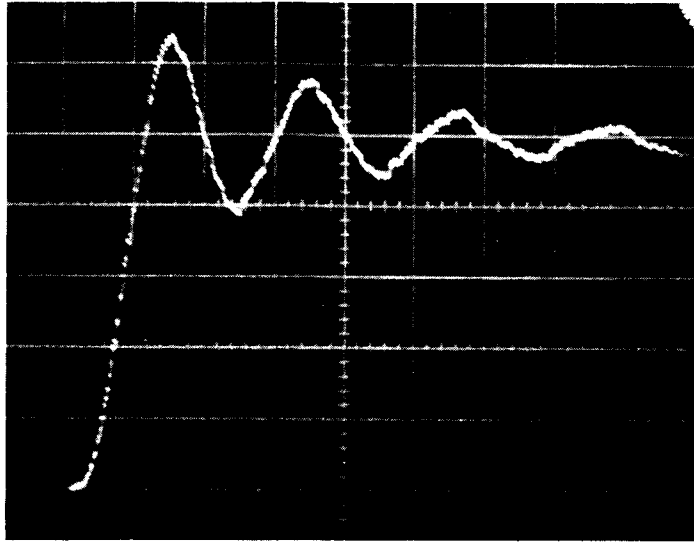


Fig. 22 Transient Response, All Channels Active  
(3.5 ma p-p, time - 0.1 sec per large div.)

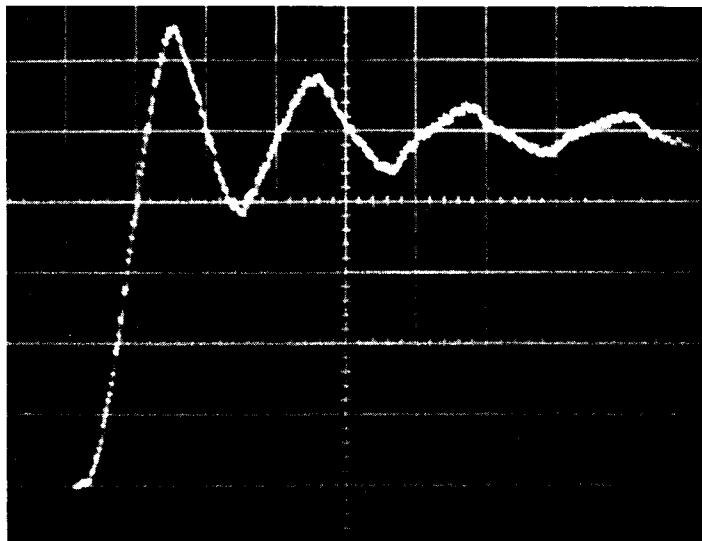


Fig. 23 Transient Response, Torque Motor #1 Failed Open  
(3.5 ma p-p, time - 0.1 sec per large div.)

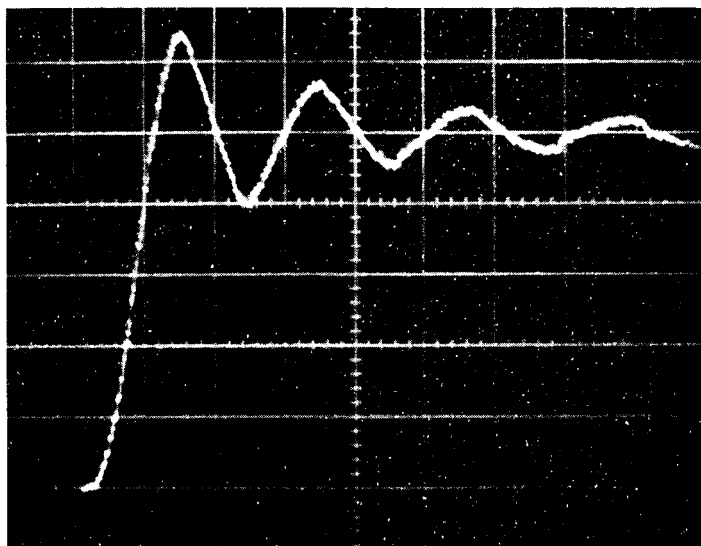


Fig. 24 Transient Response, Torque Motor #1 Failed Hard-Over  
(3.5 ma p-p, time - 0.1 sec per large div.)

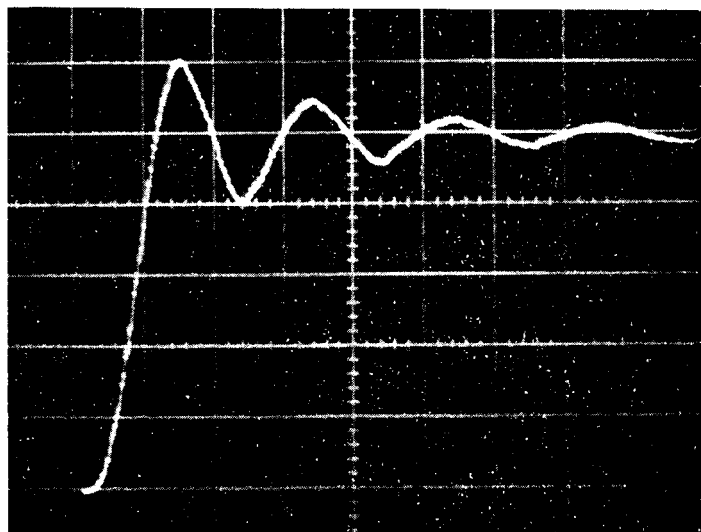


Fig. 25 Transient Response, All Channels Active  
(7.0 ma p-p, time - 0.1 sec per large div.)

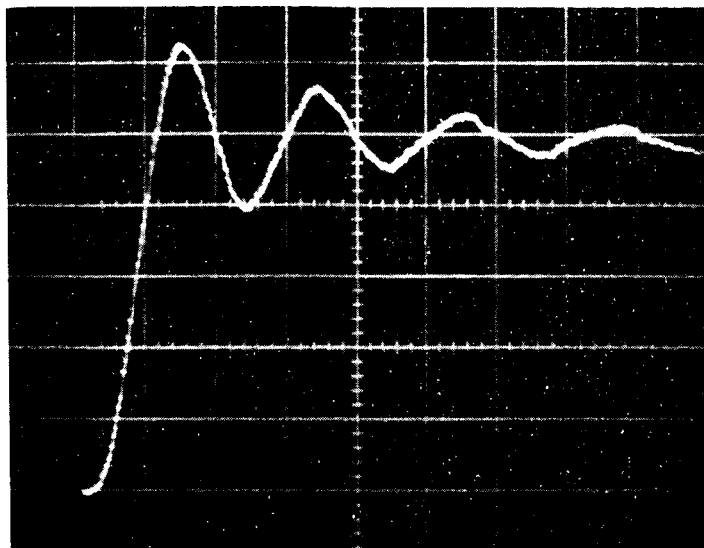


Fig. 26 Transient Response, Torque Motor #1 Failed Open  
(7.0 ma p-p, time - 0.1 sec per large div.)

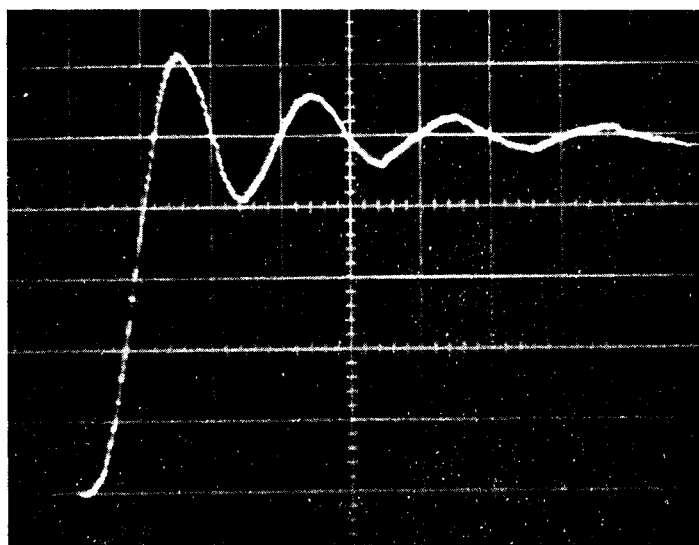


Fig. 27 Transient Response, Torque Motor #1 Failed Hard-Over  
(7.0 ma p-p, time - 0.1 sec per large div.)



Temperature testing indicated less than 5% change in actuator position up to 275°F. Throughout the test program there was no evidence of abnormal or unstable performance of the servoactuators.

## APPENDIX

- I      Performance Productions and Sizing Calculations Report,  
ER-88.
  
- II     Revised Performance Productions, ER-88A.

ENGINEERING REPORT NO. ER-88

Moog Servocontrols, Inc.      East Aurora, New York

---

TITLE:

Performance Predictions and Sizing Calculations for Moog  
Model 17-204 Actuator; Mechanical Feedback Servoactuator  
with Majority Voting Valve.

BY: D. Gusakov      AND      B. H. Weyman

DATE:    October 9, 1964

---

REFERENCES:

- (1)    Proposal for Moog Model 17-204, Majority Voting Mechanical Feedback Servoactuator for the Saturn S-IV B. (Dated 5-5-64)
- (2)    Moog Servocontrols, Inc. Engineering Report No. ER-67, "Performance Predictions and Sizing Calculations for Saturn S-IV B TVC System: 17-189 Actuator, 16-142 Valve," dated August 22, 1963
- (3)    Moog Servocontrols, Inc. Engineering Report No. ER-67A, "Revision of Engineering Report ER-67 to reflect specification changes resulting from S-IV B Design Review Meeting on September 11 and 12, 1963," dated September 24, 1963
- (4)    Moog Servocontrols, Inc. Engineering Report No. ER-67B, "Revision of Engineering Report ER-67A to reflect changes resulting from revised S-IV B actuator specification, Revision F," dated April 2, 1964

SECTION 1.0: Summary

This report summarizes the performance predictions and sizing calculations for the Moog Servoactuator Model 17-204 to be supplied to the George C. Marshall Space Flight Center, National Aeronautics and Space Administration, Huntsville, Alabama. The design provides mechanical piston position feedback and a majority voting mechanical feedback servovalve. Where possible, the design has been patterned about the Saturn S-IV B Servoactuator and associated load characteristics (Moog Model 17-189 Servoactuator).

Section 2.0 contains a summary of the pertinent system parameters; and section 3.0 shows calculations of the various loop gains and sensitivities. Figure B illustrates the system function diagram of the unit.

SECTION 2.0: Summary of System Parameters

<u>Symbol</u>	<u>Description</u>	<u>Value</u>
$A_1$	DPF piston stub areas	$0.1295 \text{ in}^2$
$A_2$	DPF piston nozzle driving areas	$0.6560 \text{ in}^2$
$A_{act}$	actuator area	$11.78 \text{ in}^2$
$D_N$	DPF nozzle diameters	$0.028 \text{ in}$
$k_{\text{feedback spring - 1}}$	Feedback spring stiffness Torque motor No. 1	$29.3 \text{ lb/in.}$
$k_{\text{feedback spring - 2}}$	Feedback spring stiffness Torque motor No. 2	$54.2 \text{ lb/in.}$
$k_{\text{feedback spring - 3}}$	Feedback spring stiffness Torque motor No. 3	$29.3 \text{ lb/in.}$
$k_{\text{sfw-1}}$	Spring rate of spool feedback wire Torque motor No. 1	$9.5 \text{ lb/in.}$
$k_{\text{sfw-2}}$	Spring rate of spool feedback wire Torque motor No. 2	$9.5 \text{ lb/in.}$
$k_{\text{sfw-3}}$	Spring rate of spool feedback wire Torque motor No. 3	$9.5 \text{ lb/in.}$
$K_3$	DPF pressure feedback slope	$0.015 \text{ cis/psi}$
$K_{cam}$	feedback cam slope	$0.04366 \text{ in/in.}$ $(2^\circ 30')$
$K_{DPF}$	DPF torque/pressure gain	$9.5 \times 10^{-5} \text{ in-lb/psi}$
$K_E$	combined rate of DPF springs per unit	$1000 \text{ lb/in.}$
$K_M$	actuator mechanical stiffness (calculated from specification parameters)	$4,760,000 \text{ lb/in.}$
$K'_M$	estimated actual actuator mechanical stiffness	$2,500,000 \text{ lb/in.}$

<u>Symbol</u>	<u>Description</u>	<u>Value</u>
$K_{oil}$	actuator oil stiffness	3,390,000 lb/in.
$K_s$	structural spring rate	391,000 lb/in.
$K_{spool}$	valve spool gain - flow per displacement	2,180 in <sup>3</sup> /sec/in.
$K_T$	total drive stiffness (calculated from specification parameters)	350,000 lb/in.
$K_T'$	estimated total drive stiffness	307,000 lb/in.
$K_{TM-1}$	gain of torque motor No. 1	0.046 in-lb/ma
$K_{TM-2}$	gain of torque motor No. 2	0.046 in-lb/ma
$K_{TM-3}$	gain of torque motor No. 3	0.046 in-lb/ma
$K_{valve}$	valve flow per torque gain	158 cis/in-lb.
$K_{vp}(DPF)$	dynamic pressure loop gain	33.2 sec <sup>-1</sup>
$K_{vx}$	positional loop gain	20 sec <sup>-1</sup>
$l$	total actuator stroke	2.5 in.
$l_{feedback\ spring-1}$	length from feedback spring input to torque motor flexure point Torque motor No. 1	1.16 in.
$l_{feedback\ spring-2}$	length from feedback spring input to torque motor flexure point Torque motor No. 2	0.625 in.
$l_{feedback\ spring-3}$	length from feedback spring input to torque motor flexure point Torque motor No. 3	1.16 in.
$l_{sfw-1}$	length from spool displacement pickup point to torque flexure point Torque motor No. 1	1.45 in.
$l_{sfw-2}$	length from spool displacement pickup point to torque flexure point Torque motor No. 2	1.45 in.

<u>Symbol</u>	<u>Description</u>	<u>Value</u>
$l_{\text{sfw-3}}$	length from spool displacement pickup point to torque flexure point Torque motor No. 3	1.45 in.
$M_E$	equivalent reflected engine mass	120 lb-sec <sup>2</sup> /in.
$N$	volumetric efficiency factor (assumed)	0.9 (dimensionless)
$X_{\text{DPF}}$	DPF nozzle spacing from flapper	0.0012 in.
$\beta$	bulk modulus of MIL-H-5606 oil	200,000 lb/in <sup>2</sup>
$\tau_o$	DPF time constant	0.08 sec. at $\pm 200$ psi load $\Delta P$
$\omega_E$	natural frequency of mass and effective oil-structure spring (specification value)	54 rad/sec.
$\omega'_E$	natural frequency of mass and effective oil-structure spring (calculated from estimated parameters)	53.4 rad/sec.
$\omega_s$	natural frequency of mass and structure spring	57.1 rad/sec.
	actuator sensitivity	0.031 in/ma
	rated command current	50 ma
	rated valve flow	10.5 gpm at 3500 psi $\Delta$ valve
	stroke of DPF piston	$\pm 0.26$ in.
	actuator attach radius	11.87 inches
	engine gimballing inertia	1450 slug-ft <sup>2</sup>
	valve spool diameter	0.375 inch

### SECTION 3.0: Loop Gain and Sensitivities

Each of the three mass balanced -2 series torque motors has a nominal rated output of:

$$\begin{aligned}
 \text{Max. output torque} &= (K_{TM}) (\text{rated current}) \\
 &= (0.046 \text{ in-lb/ma}) (50 \text{ ma}) \\
 &= 2.3 \text{ in-lb.}
 \end{aligned}$$

The actuator ram position sensitivity to current input is nominally the same for each channel. While the actuator stroke is less than the S-IV B 17-189 unit, the sensitivity has been designed to be identical. Thus the piston will bottom before rated current. For channel -1:

$$\begin{aligned}
 \text{Actuator Sensitivity} &= \frac{(K_{TM-1})}{(K_{cam}) (k_{\text{feedback}}) (l_{\text{feedback}})} \\
 &\quad \text{spring - 1} \quad \text{spring - 1} \\
 &= \frac{0.046}{(0.04366) (29.3) (1.16)} \\
 &= 0.031 \text{ in/ma}
 \end{aligned}$$

The position loop gain ( $K_{vx}$ ) is nominally the same for each channel. For channel -1:

$$\begin{aligned}
 K_{vx} &= \frac{K_{spool} K_{cam} k_{\text{feedback}} l_{\text{feedback}}}{A_{act} l_{sfw-1} k_{sfw-1}} \\
 &= \frac{(2180) (0.04366) (29.3) (1.16)}{(11.78) (1.45) (9.5)} \\
 &= 20 \text{ sec}^{-1}
 \end{aligned}$$

The dynamic pressure loop gain  $K_{vp}$ (DPF) is nominally the same for each channel. For channel -1:



$$\begin{aligned} K_{vp}(\text{DPF}) &= \frac{K_{\text{spool}} K'_T K_{\text{DPF}}}{A_{\text{act}}^2 \ell_{\text{sfw}} - 1 k_{\text{sfw}} - 1} \\ &= \frac{(2180) (307,000) (9.5 \times 10^{-5})}{(11.78)^2 (1.45) (9.5)} \end{aligned}$$

The Moog servosystem analyzer was programmed to simulate the engine - stage structure characteristics of the Saturn S-IV B TVC and the 17-204 actuator, according to the nominal parameters as listed on Figure A. Step and frequency response data was taken and are presented in Figures A and AA respectively.

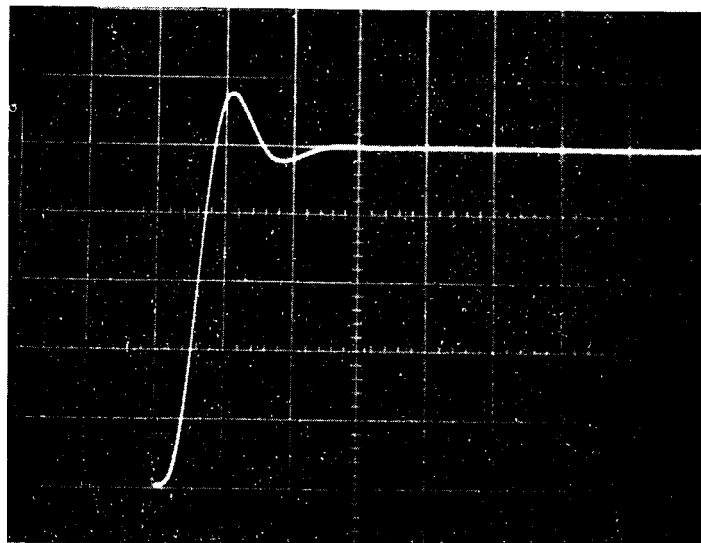


FIGURE A

Moog Model 17-204

Analog Computer Simulation of:

Engine Position Response to Step Command

All System Parameters Nominal as Follows:

Drive-Load Resonant Frequency =  $\omega_e = 53.4$  rad/sec.

Structure-Load Resonant Frequency =  $\omega_s = 57.1$  rad/sec.

Drive-Load Damping Ratio =  $\zeta_e = 0$

Positional Loop Gain =  $K_{vx} = 20 \text{ sec}^{-1}$

Dynamic Pressure Loop Gain =  $K_{vp}(\text{DPF}) = 33.2 \text{ sec}^{-1}$

DPF Time Constant =  $\tau_o = 0.08 \text{ sec}$  at  $\pm 200 \text{ psi}$  load  $\Delta P$

Servovalve dynamics: second order with a resonant frequency of 50 cps and a damping ratio of 1.0

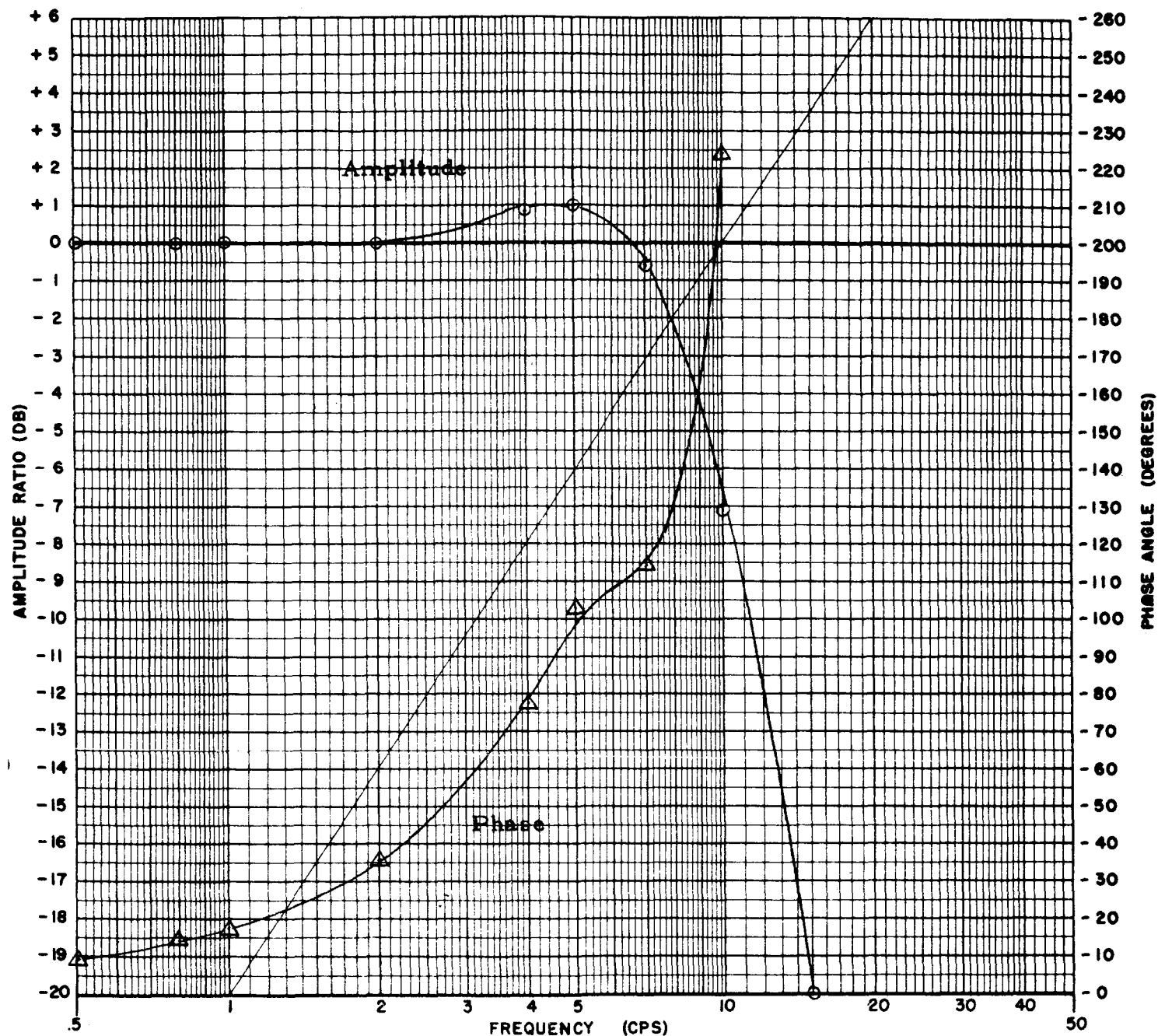
Feedback from piston position

Single Sweep at 0.1 sec/cm

# SERVOACTUATOR DYNAMIC RESPONSE

ER-88

Page 9



MODEL 17-204 SERIAL \_\_\_\_\_

DATE 8/26/64 BY IG/AH

SYSTEM PRESSURE \_\_\_\_\_ PSI

INPUT SIGNAL Command ( $\beta_i$ ) MA.(P-P)

OUTPUT Engine Position ( $\beta_e$ )

FIGURE AA

Analog Computer Simulation - Mechanical Feedback Servoactuator with Majority-Voting Valve.

**MOOG SERVOCONTROLS, INC.**  
EAST AURORA, NEW YORK

All parameters as listed on Figure A.



ENGINEERING REPORT NO. ER-88A

Moog Servocontrols, Inc. East Aurora, New York

---

TITLE:

Revision of Engineering Report ER-88 to Reflect  
Specification Changes of the Moog Model 17-204  
Mechanical Feedback Actuator with Majority Voting  
Valve

BY: I. Gusakov  
Ignaty Gusakov

APPROVED: B. H. Weppner  
B. H. Weppner

DATE: December 22, 1964

---

REFERENCE:

Moog Servocontrols, Inc. Engineering Report No.  
ER-88, "Performance Predictions and Sizing  
Calculations for Moog Model 17-204 Actuator;  
Mechanical Feedback Servoactuator With Majority  
Voting Valve"

SECTION 1.0

## Introduction

This report summarizes the new performance predictions and system parameters of the Moog Model 17-204 servoactuator. The new performance predictions and system parameters reflect a lowering of the load mass and structure spring natural frequency ( $\omega_s$ ) from 57.1 rad/sec to 43.0 rad/sec and a lowering of the position loop gain ( $K_{vx}$ ) from 20.0 sec<sup>-1</sup> to 14.25 sec<sup>-1</sup>.

Section 2.0 contains a summary of the pertinent system parameters. Section 3.0 shows the necessary calculations for determining values of the parameters which were affected by the above mentioned changes in  $\omega_s$  and  $K_{vx}$ .



SECTION 2.0: Summary of System Parameters

<u>Symbol</u>	<u>Description</u>	<u>Value</u>
$A_1$	DPF piston stub areas	0.1295 in <sup>2</sup>
$A_2$	DPF piston nozzle driving areas	0.6560 in <sup>2</sup>
$A_{act}$	Actuator area	11.78 in <sup>2</sup>
$A_N$	Valve nozzle areas	0.000201 in <sup>2</sup>
$D_N$	DPF nozzle diameters	0.038 in
$k_{B-1}$	Effective Bernoulli spring rate Torque motor No. 1	1.72 lb/in
$k_{B-2}$	Effective Bernoulli spring rate Torque motor No. 2	1.72 lb/in
$k_{B-3}$	Effective Bernoulli spring rate Torque motor No. 3	1.72 lb/in
$k_{feedback}$ spring-1	Feedback spring stiffness Torque motor No. 1	29.3 lb/in.
$k_{feedback}$ spring-2	Feedback spring stiffness Torque motor No. 2	54.2 lb/in.
$k_{feedback}$ spring-3	Feedback spring stiffness Torque motor No. 3	29.3 lb/in.
$k_{sfw-1}$	Spring rate of spool feedback wire Torque motor No. 1	12.4 lb/in
$k_{sfw-2}$	Spring rate of spool feedback wire Torque motor No. 2	12.4 lb/in
$k_{sfw-3}$	Spring rate of spool feedback wire Torque motor No. 3	12.4 lb/in
$K_3$	DPF pressure feedback slope	0.015 cis/psi
$K_{cam}$	Feedback cam slope	0.04366 in/in (2° 30')

<u>Symbol</u>	<u>Description</u>	<u>Value</u>
$K_{DPF}$	DPF torque/pressure gain	$13.3 \times 10^{-5}$ in-lb/psi
$k_E$	Combined rate of DPF springs per unit	479 lb/in
$k_M$	Estimated actual actuator mechanical stiffness	2,500,000 lb/in
$k_{oil}$	Effective actuator oil stiffness	3,390,000 lb/in
$k_s$	Effective structural spring rate	222,000 lb/in
$K_{spool}$	Valve spool gain - flow per displacement	$2,180 \text{ in}^3/\text{sec/in}$
$k_T$	Estimated total drive stiffness	192,000 lb/in
$K_{TM-1}$	Gain of torque motor No. 1	0.046 in-lb/ma
$K_{TM-2}$	Gain of torque motor No. 2	0.046 in-lb/ma
$K_{TM-3}$	Gain of torque motor No. 3	0.046 in-lb/ma
$K_{valve}$	Valve flow per torque gain	113 cis/in-lb
$K_{vp}(DPF)$	Dynamic pressure loop gain	$20.4 \text{ sec}^{-1}$
$K_{vx}$	Positional loop gain	$14.25 \text{ sec}^{-1}$
$l$	Total actuator stroke	2.5 in
$l_{f-1}$	Length from flexure point to valve nozzles Torque motor No. 1	0.760 in
$l_{f-2}$	Length from flexure point to valve nozzles Torque motor No. 2	0.760 in
$l_{f-3}$	Length from flexure point to valve nozzles Torque motor No. 3	0.760 in
$l_{\text{feedback spring-1}}$	Length from feedback spring input to torque motor flexure point Torque motor No. 1	1.16 in

<u>Symbol</u>	<u>Description</u>	<u>Value</u>
$l_{\text{feedback spring-2}}$	Length from feedback spring input to torque motor flexure point Torque motor No. 2	0.625 in.
$l_{\text{feedback spring-3}}$	Length from feedback spring input to torque motor flexure point Torque motor No. 3	1.16 in
$l_{N-1}$	Length from flexure point to DPF nozzles Torque motor No. 1	0.580 in
$l_{N-2}$	Length from flexure point to DPF nozzles Torque motor No. 2	0.580 in
$l_{N-3}$	Length from flexure point to DPF nozzles Torque motor No. 3	0.580 in
$l_{\text{sfw-1}}$	Length from spool displacement pickup point to torque flexure point Torque motor No. 1	1.45 in.
$l_{\text{sfw-2}}$	Length from spool displacement pickup point to torque flexure point Torque motor No. 2	1.45 in.
$l_{\text{sfw-3}}$	Length from spool displacement pickup point to torque flexure point Torque motor No. 3	1.45 in.
$M_E$	Equivalent reflected engine mass	120 lb-sec <sup>2</sup> /in.
$N$	Volumetric efficiency factor (assumed)	0.9 (dimensionless)
$X_{\text{DPF}}$	DPF nozzle spacing from flapper	0.0012 in.
$\beta$	Bulk modulus of MIL-H-5606 oil	200,000 lb/in <sup>2</sup>
$\tau_o$	DPF time constant	0.132 sec at $\pm 200$ psi load $\Delta P$
$\omega_E$	Natural frequency of mass and effective oil-structure spring (calculated from estimated parameters)	40.0 rad/sec.

<u>Symbol</u>	<u>Description</u>	<u>Value</u>
$\omega_s$	Natural frequency of mass and structure spring	43 rad/sec.
	Actuator sensitivity	0.031 in/ma
	Rated command current	50 ma
	Rated valve flow	10.5 gpm at 3500 psi $\Delta$ valve
	Stroke of DPF piston	$\pm 0.26$ in.
	Actuator attach radius	11.87 inches
	Engine gimbaled inertia	1450 slug-ft <sup>2</sup>
	Valve spool diameter	0.375 inch

### SECTION 3.0:      Calculation of System Parameters

Section 3.1:      Determination of the natural frequency of mass and effective oil - structure spring ( $\omega_E$ ).

$$k_s = M_E \omega_s^2$$

$$k_s = (120) (43^2)$$

$$k_s = 222,000 \text{ lb/in.}$$

$$k_{oil} = 3,390,000 \text{ lb/in.}$$

$$k_M = 2,500,000 \text{ lb/in}$$

$$k_T = \frac{1}{\frac{1}{k_M} + \frac{1}{k_{oil}} + \frac{1}{k_s}}$$

$$k_T = \frac{1}{\frac{1}{2,500,000} + \frac{1}{3,390,000} + \frac{1}{222,000}}$$

$$k_T = 192,000 \text{ lb/in}$$

$$\omega_E = \sqrt{k_T / M_E}$$

$$\omega_E = \sqrt{\frac{192,000}{120}}$$

$$\omega_E = 40.0 \text{ rad/sec}$$

Section 3.2:      Determination of the effective Bernoulli spring rate within the servovalve.

The Bernoulli force on the valve spool  $F_B$  can be expressed by the relationship:

$$F_B = 0.45 W (P_s - P_L) X_s$$

where:

0.45 is a constant

$W = 0.6$  in. is the total slot width

$P_s = 3500$  psi is the system pressure

$P_L = 0$  is the load pressure drop

$X_s$  is the spool position.

The torque on the armature,  $T_B$ , due to the change in pressure across the nozzles caused by the Bernoulli force on the spool is:

$$T_B = \frac{F_B A_N l_f}{A_s}$$

where:

$A_N = 0.000201$  in<sup>2</sup> is the nozzle area

$A_s = 0.1104$  in<sup>2</sup> is the spool area

$l_f = 0.76$  in. is the distance from the flexure point to the nozzles or the Bernoulli moment

Assuming that  $P_L = 0$ ,

$$T_B = \frac{0.45 W P_s X_s A_N l_f}{A_s}$$

$$\frac{T_B}{X_s} = \frac{(0.45)(0.6)(3500)(0.000201)(0.76)}{0.1104}$$

$$\frac{T_B}{X_s} = 1.307 \frac{\text{in-lb}}{\text{in}}$$

$$k_B = \frac{F_B}{X_s}$$

$$k_B = \frac{T_B}{X_s l_f}$$

$$k_B = \frac{1.307}{0.76}$$



$$k_B = 1.72 \text{ lb/in}$$

The effect of this spring rate adds to that of the spool feedback wire rate of the valve. This is shown on the block diagram of Figure B.  $k_B$  and  $l_f$  have the same values for each of the three servovalves.

### Section 3.3: Determination of the spool feedback wire rate, $k_{sfw}$

The position loop gain  $K_{vx}$  is defined by:

$$K_{vx} = \frac{K_{spool} K_{cam} k_{fbs} l_{fbs}}{A_{act} (k_{sfw} l_{sfw} + k_B l_f)}$$

$$k_{sfw} = \frac{K_{spool} K_{cam} k_{fbs} l_{fbs}}{K_{vx} A_{act} l_{sfw}} - \frac{k_B l_f}{l_{sfw}}$$

$$k_{sfw} = \frac{(2180)(0.04366)(29.3)(1.16)}{(14.25)(11.78)(1.45)} - \frac{(1.72)(0.76)}{1.45}$$

$$k_{sfw} = 13.31 - 0.90$$

$$k_{sfw} = 12.4 \text{ lb/in.}$$

$k_{sfw}$  has the same value for all three servovalves.

### Section 3.4: Determination of the dynamic pressure loop gain $K_{vp}^{DPF}$ .

$$K_{vp} = \frac{K_3 k_T}{A_{act}^2}$$

$$K_{vp} = \frac{(0.015)(192,000)}{11.78^2}$$

$$K_{vp} = 20.4 \text{ sec}^{-1} \text{ for each of the three loops}$$

Section 3.5: Determination of the valve flow per torque gain,  $K_{\text{valve}}$ .

$$K_{\text{valve}} = \frac{K_{\text{spool}}}{k_{\text{sfw}} \ell_{\text{sfw}} + k_B \ell_f}$$

$$K_{\text{valve}} = \frac{2180}{(12.4)(1.45) + (1.72)(0.76)}$$

$K_{\text{valve}} = 113 \text{ cis/in-lb}$  for each of the three servovalves.

Section 3.6: Determination of the DPF torque per pressure gain,  $K_{\text{DPF}}$ .

$$K_{\text{DPF}} = \frac{K_3 (k_{\text{sfw}} \ell_{\text{sfw}} + k_B \ell_f)}{K_{\text{spool}}}$$

$$K_{\text{DPF}} = \frac{(0.015) [(12.4)(1.45) + (1.72)(0.76)]}{2180}$$

$$K_{\text{DPF}} = 13.3 \times 10^{-5} \text{ in-lb/psi}$$

Section 3.7: Determination of the DPF nozzle diameter,  $D_N$ .

$$D_N = \sqrt{\frac{4 K_3 A_2}{\pi \ell_N K_{\text{valve}} A_1}}$$

$$D_N = \sqrt{\frac{(4)(0.015)(0.656)}{\pi (0.580)(113)(0.1295)}}$$

$$D_N = 0.038 \text{ in}$$

Section 3.8: Determination of the combined rate of the DPF springs,  $k_E$ .

From Figure C, the nominal DPF time constant is

$$\tau_o = 0.132 \text{ sec.}$$

$$k_E = \frac{2A_2^2 \sqrt{\left(\frac{A_1}{A_2}\right) \Delta P_{LO}}}{(3)(209) \pi D_N X_{DPF} \tau_o} \quad \text{where: } \Delta P_{LO} = 200 \text{ psi}$$

$$k_E = \frac{(2)(0.656)^2 \sqrt{\left(\frac{0.1295}{0.656}\right) (200)}}{(3)(209) \pi (0.038)(0.0012)(0.132)}$$

$$k_E = 479 \text{ lb/in}$$

Section 3.9: Determination of the static pressure which will cause bottoming of the DPF piston.

$$\begin{aligned} \Delta P &= \frac{k_E X_p}{A_1} \\ &= \frac{(479 \text{ lb/in})(\pm 0.26 \text{ in})}{(0.1295)} \\ &= \pm 960 \text{ psi} \end{aligned}$$

The Moog servosystem analyzer was programmed to simulate the engine-stage structure characteristics of the Saturn S-IVB TVC and the 17-204 actuator according to the current nominal parameters which are listed in Figure A. Step and frequency response data were taken and are presented in Figures A and AA respectively.

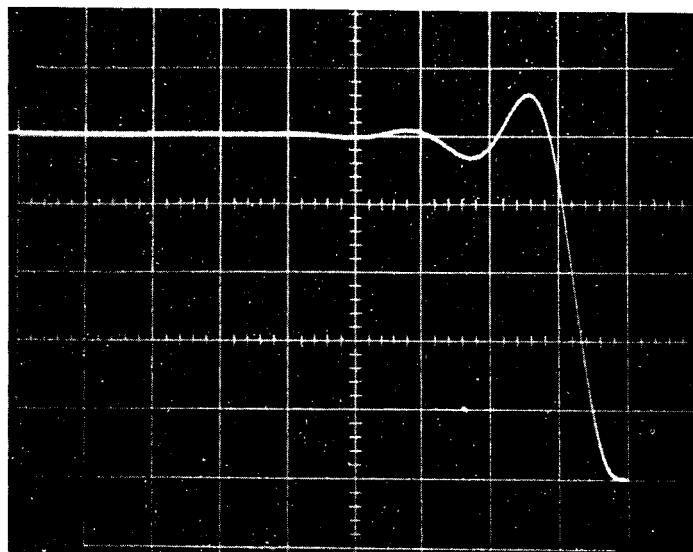


FIGURE A

**Moog Model 17-204 Servoactuator****Analog Computer Simulation of:****Engine Position Response to Step Command****All System Parameters Nominal as Follows:****Drive - Load Resonant Frequency  $= \omega_E = 40.0 \text{ rad/sec}$** **Structure - Load Resonant Frequency  $= \omega_s = 43.0 \text{ rad/sec}$** **Drive - Load Damping Ratio  $= \zeta_e = 0$** **Position Loop Gain  $= K_{vx} = 14.25 \text{ sec}^{-1}$** **Dynamic Pressure Loop Gain  $= K_{vp} \text{ (DPF)} = 20.4 \text{ sec}^{-1}$** **DPF Time Constant  $= \tau_o = 0.132 \text{ sec}$  at  $\pm 200 \text{ psi load } \Delta P$** **Servo valve Dynamics: Second Order with a Resonant Frequency of 50 cps and a damping ratio of 1.0****Feedback From Piston Position****Single Sweep at 0.1 sec/cm**

## SERVOACTUATOR DYNAMIC RESPONSE

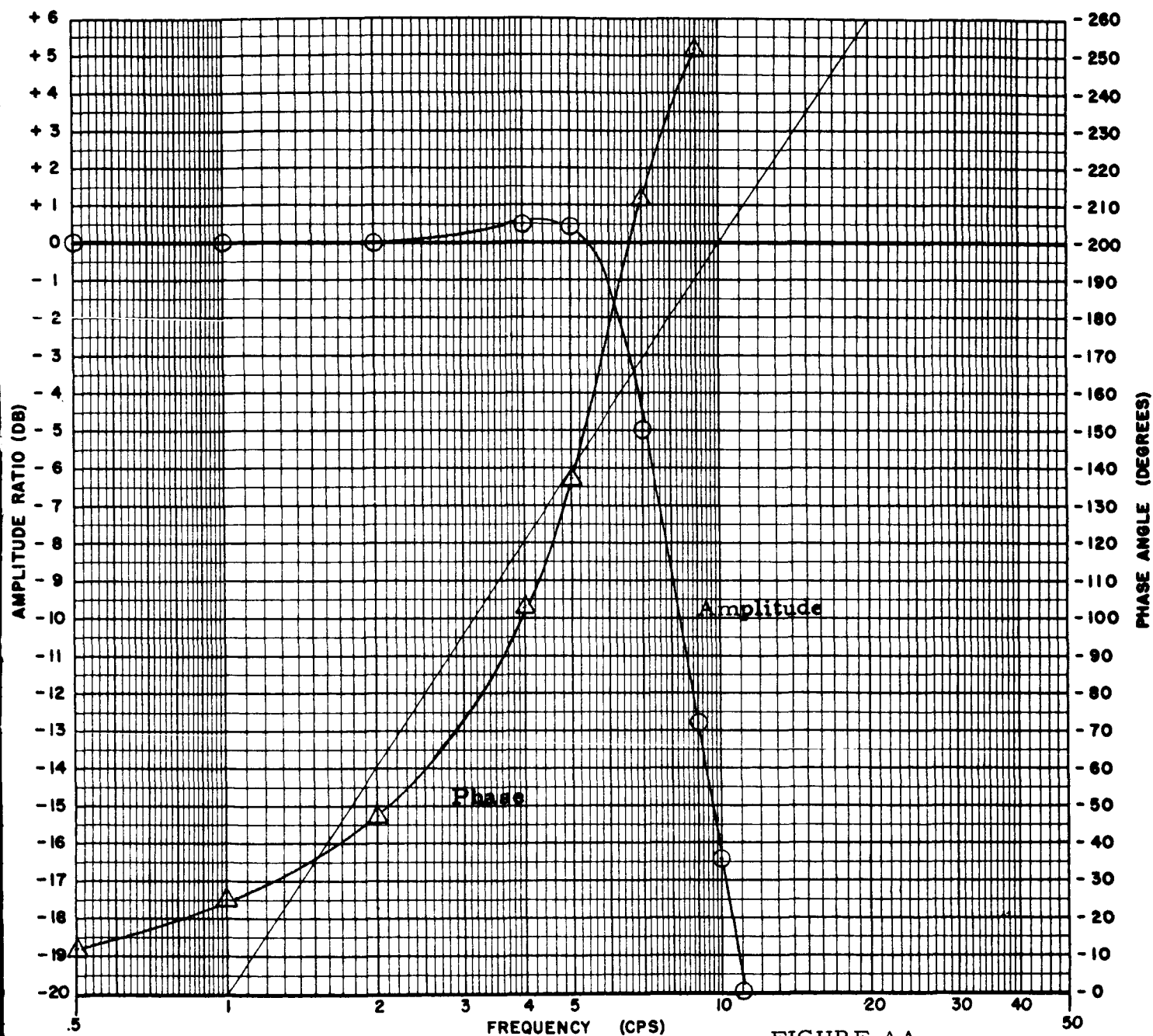


FIGURE AA

Analog Computer Simulation - Mechanical Feedback Servoactuator With Majority - Voting Valve.

MODEL 17-204 SERIAL \_\_\_\_\_

DATE 12/19/64 BY \_\_\_\_\_

SYSTEM PRESSURE \_\_\_\_\_ PSI

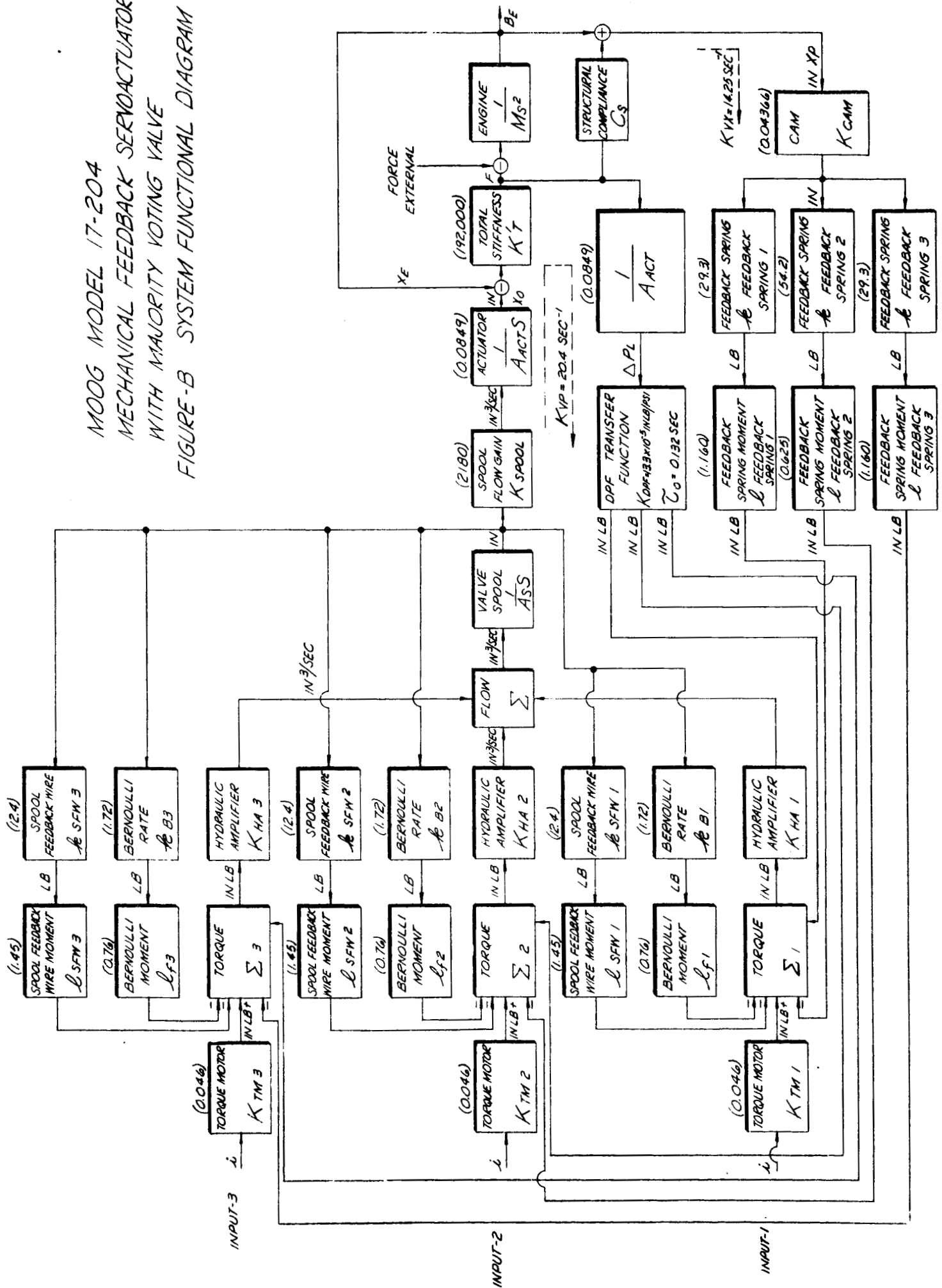
INPUT SIGNAL Command ( $\theta_i$ ) MA.(P-P)

OUTPUT Engine Position ( $\theta_o$ )

**MOOG SERVOCONTROLS, INC.**  
EAST AURORA, NEW YORK

All parameters as listed on Figure A

MOOG MODEL 17-204  
MECHANICAL FEEDBACK SERVOACTUATOR  
WITH MAJORITY VOTING VALVE  
FIGURE-B SYSTEM FUNCTIONAL DIAGRAM





16-142

DPF Corner Frequency Test Requirements

S/N

Date

3500 psi system

Valve adjusted to maintain #200 psi load ΔP

FIGURE C

 $f_0 = 1.21 \text{ cps}$ ,  $\tau_0 = 0.132 \text{ sec}$ 